GALILEAN SATELLITE OBSERVATION PLANS FOR THE NEAR INFRARED MAPPING SPECTROMETER EXPERIMENT ON THE GALILEO SPACECRAFT

W.D. Smythe (l), R. Lopes-Gautier (l), A. Ocampo (l), J. Hui (l), M. Segura (l), L.A. Soderblom (2), D.L. Matson (l), H.H. Kieffer (2), T.B. McCord (3, 4), F.P. Fanale (3), W.M. Calvin (2), J. Sunshine (4), E. Barbinis (5), R.W. Carlson (l), and P.R. Weissman (1)

(1) Jet Propulsion Laboratory, California Institute of Technology, 4800 Oak Grove Drive, Pasadena, CA 91109

(2) U.S. Geological Survey, Branch of Astrogeologic Studies, 2255 N. Gemini Drive, Flagstaff, AZ 86001

(3) University of Hawaii, Planetary Geoscience Division, 2525 Correa Road, Honolulu, HI 96822

(4) SETS Technology, Inc., 300 Kahelu Ave, suite 10, Mililani, HI 96789

(5) Institute of Geophysics and Planetary Physics, University of California at Los Angeles, 405 Hilgard Ave, Los Angeles, CA 90024

Journal of Geophysical Research, in press

ABSTRACT:

On December 7, 1995 the Galileo spacecraft will begin observations of the Jovian system with orbit insertion and a satellite tour of 10 orbits. The Galilean satellites will be observed with four remote sensing instruments spanning the ultraviolet, visible, near infrared and thermal infrared regions of the spectrum. The Galileo Near-Infrared Mapping Spectrometer will observe the satellites in the wavelength range 0.7 to 5.2 microns - a region particularly well-suited for analyzing volatile components. Planned observations include mapping most available longitudes at about 100 km resolution per pixel at full wavelength resolution, together with observing limited regions at high spatial resolution. The opportunity to af feet the choice and design of observations for the Galileo tour extends until June 1996.

1. Introduction

In December 1995, the Galileo spacecraft will commence a two year investigation of the Jovian system including the magnetosphere, Jupiter's atmosphere, and the Galilean satellites: Io, Europa, Ganymede, and Callisto. Included in the scientific instrument complement of Galileo is the Near Infrared Mapping Spectrometer (NIMS), which is specifically designed for remote sensing studies of these diverse moons of Jupiter. Although the total volume of data that will be returned during the mission is less than originally planned, due to the functional loss of the high gain antenna, we anticipate return of a wealth of new, first-of-its-kind spatially resolved near infrared data, providing a comprehensive understanding of the surface composition and evolution of the Galilean satellites. Accomplishing this with restricted data return requires careful planning and design of the observations and requires making difficult choices between the number and types of observations. The purpose of this paper is to present our current plans and goals for satellite observations with NIMS to the scientific communit y and to solicit suggestions for important observations that should be included.

NIMS utilizes a combination of two remote sensing techniques: imaging and spectroscopy. This powerful combination allows one to map distinct units on the surfaces and, through spectroscopic measurements, to identify significant materials such as mafic minerals and clays present in these units.

Localized species, whose contribution to the whole-disc spectra can be too weak to observe, are investigated through high spatial resolution observations. The entire surface of a satellite cannot be mapped at the highest possible spatial and spectral resolution, so tradeoffs between global coverage and high spatial resolution regional coverage have been made. Our general philosophy is to perform complete global spectral mapping at modest spatial and high spectral resolution for each of the satellites. These primary data sets are obtained in a consistent manner for all of the satellites, enabling comparisons between the satellites. For the remainder of the data, limited numbers of high spatial resolution measurements will be performed for specific localized targets. The choice of these targets depends partly upon tour opportunities and observation geometry, and partly upon perceived scientific benefit and value.

2. The NIMS Instrument

The NIMS instrument has been described previously by Carl son et al. (1992); its basic operation is only briefly outlined here. NIMS (Fig. 1) includes a 23 cm aperture telescope with a scanning secondary mirror, a spectrometer with a scanning grating and a focal plane array mounted on a radiative cooler. NIMS forms spectra with the moving grating in combination with 17 detectors (2 Si, 15 InSb) spaced approximately evenly in wavelength. Various spectral sampling densities are achieved by varying the step size for the grating. The number of grating positions per cycle ean vary from 1 to 24, resulting in spectral sampling of 17 to 408 wavelengths across the spectral range of the instrument (0.7 to 5.2 microns). The spectral resolution is 0.026 microns FWHM (0.013 at wavelengths $<$ 1 micron). The minimum grating step size is one half of a wavelength resolution element. Standard instrument modes include grating step increments of 1,2,4, and O grating positions - with the corresponding number of wavelength samples being 408, 204, 102, and 17. The corresponding mode names are Long Map (LM), Full Map (FM), Short Map (SM), and Fixed Map (XM), respectively. The NIMS instrument response is depicted in Figure 2 and examples of spectra taken by NIMS are shown in Figure 3.

To fit within limited telemetry capabilities, several modifications have been made to the

capabilities of the instrument and the command data system (CDS) of the spacecraft. These changes permit editing of the instrument data stream to select any subset of wavelengths from a given instrument mode. A general data return strategy will be to edit data within the instrument to just fit within (fully utilize) the fixed-size allocations on the spacecraft tape recorder. Further wavelength editing will occur in CDS prior to data transmission to Earth in order to fit within the available telemetry bandwidth. This strategy permits a modest adaptability in the choice of returned wavelengths, which is important for responding to the discovery of new spectral features for the satellites and atmospheres.

3. Scientific Background and Objectives

Galileo will be the first spacecraft to orbit Jupiter. Galileo's tour (described by Wolf and Byrnes, 1993) will consist of 11 orbits (Fig. 4), which are designed to optimize close encounters with Europa, Ganymede, and Callisto, and to enable studies of Jupiter's atmosphere and magnetosphere. The tour's highlights and the major science objectives for each orbit are given in Table 1.

This will be the first time that the Galilean satellites will be observed in the wavelength region 0.7 - 5.2 microns without atmospheric interference and at spatial resolutions higher than 1000 km/pixel. The higher spatial resolution for this wavelength region, which for NIMS averages about 80 km/pixel, with highest resolution of 1 km/pixel, permits detection of minor species whose spectral signatures may not be apparent in the global averages obtainable from Earth. The higher spatial resolution obtainable by NIMS is particularly important for the detection of volatiles trapped at the poles and contained in localized areas on the satellites.

The NIMS wavelength range is particularly useful for detecting the condensed volatiles which tend to have strong bands in the 1.6 to 4.5 micron region. The guest molecules in clathrate structures can be detected if their absorption bands lie outside the saturated absorption bands for water ice. The OH bands associated with hydrated minerals such as clays can be distinguished from water ice in this wavelength range in the 2 to 3 micron region. Iron bands for olivine, pyroxene, and plagioclase can be detected in the 0.9 to 2.5 micron region. The distribution of SO_2 can be monitored on 10 utilizing

the well-known 4.1 micron band, a band which is also expected to be relevant for the trailing side of Europa, The NIMS wavelength region is also suitable for measuring the temperature of objects as cold as 180 K. The ability to acquire both color and brightness temperatures enables measurements both of the temperature and of the areal extent of thermal anomalies. Since the Galilean satellites have equilibrium subsolar surface temperatures of about 140 K, all temperature anomalies measured by NIMS will be endogenic.

Figure 5 shows laboratory spectra of a variety of potential materials convolved to NIMS resolution as planned for the global mosaics (see next section). This figure demonstrates the abundant spectral variability of potential materials as well as the ability of NIMS to discriminate among them.

3.110

Io offers a unique opportunity for the study of planetary volcanism at both large-scale (interior dynamics) and small scale (modelling of flows and plumes). One of the primary objectives of the Galileo mission is to investigate Io's volcanism and its interaction with Jupiter's magnetosphere. While the enormous extent of Io's volcanic activity was established by Voyager data (e.g. Morabito et al. 1979; Hanel et al. 1979; Smith et al. 1979) and subsequent ground-based infrared observations (e.g. Johnson et al. 1984; Goguen et al. 1988; Veeder et al. 1994), many important questions remain, such as the relative roles of silicates and sulfur in the composition of Io's upper crust and volcanic melts.

Arguments favoring a composition predominantly of sulfur are based on spectral data [e.g. Wamsteker et al. 1974; Fanale et al. 1979], on temperature measurements by Voyager (which indicated maximum temperatures of about 600 K) and on the surface colors shown by Voyager images [Sagan 1979; Pieri et al. 1984]. However, the evidence from surface colors has been strongly disputed [e.g. Young 1984; Gradie and Moses 1983; Nash 1987] and some ground-based temperature measurements (some over 1000 K, Matson et al. 1994) suggest that silicate volcanism is taking place [e.g. Johnson et al. 1988; Veeder et al. 1994; Blaney et al. 1994]. A predominantly silicate composition is also strongly supported by the topography of some of 10's features [Clew and Carr 1980; Moore et al. 1986] and by Io*s density, which is similar to that of the Earth's moon.

Evidence for the presence of sulfur compounds on 10's surface comes from ground based spectral data which, together with laboratory experiments, show that SO_2 frost is a component of the surface of 10 (Smythe et al. 1979; Fanale et al. 1979; Hapke 1989). The distribution of SO_2 frost on the surface has been mapped by Howell et al. (1984), using the IR band at 4.1 microns, and by Nelson et al. [1980] using the UV band (0.28 microns). Evidence for the presence of SO_2 in Io*s atmosphere was obtained by the Voyager IRIS experiment, which detected SO_2 gas over the erupting Loki volcano (Pearl et al, 1979). Rotational lines from an SO_2 atmosphere have been detected in the microwave observations of Lellouch et al. (1992). In addition, ionized sulfur has been detected in the Io torus (Broad foot et al. 1979). The presence of H_2S [Nash and Howell 1989; Salama et al 1990] and of Na_2S and Na_2O_2 [Nash 1993] has also been suggested. Tentative identifications of various other sulphur compounds, including SO_3, Na_2SO_3, and $NaHSO_4$, have been made by Khanna et al. [1993].

It is very likely that both sulfur and silicates are present on Io but their location on the surface, relative abundance, and temporal changes are unknown. Also, the composition of the lava flows on 10 is still controversial. One of NIMS' primary objectives is to identify these components and map their locations on the surface and any temporal variations. NIMS may also locate still unknown spectral features and confirm the exi stence of others (such as H_2S).

The source, density, and horizontal distribution of gaseous SO_2 in Io's atmosphere need to be investigated. Current models for atmospheric SO_2 origin can be roughly classified as one of three types: buffered, volcanic, or sputtered [Lellouch et al. 1992]. Recent millimeter-wave observation results, which allowed the first ground-based detection of Io's atmosphere [Lellouch et al. 1992], favor the volcanic model, but stress that aspects of all three types of models are probably at work on Io. NIMS will make observations of Io's atmosphere which arc designed to clarify the relative importance of these various processes.

The frequency and rate of Io's volcanic activity need to be determined more precisely. NIMS observations during the two-year satellite tour will monitor the frequency of 10's eruptions and measure the temperatures of hot spots and outbursts. These measurements will be used to refine values

for Io's mean heat flow, which is currently estimated at 2 +/- 1 W/m* [Matson et al. 1981]. The level of Io's heat flow is dependent upon the tidal dissipation properties of Io and Jupiter and is a key parameter which constrains models of Io, Jupiter, and the dynamical interactions in the Jovian system [e.g. Greenberg 1989].

Recent work by Veeder et al. [1994] has identified a "thermal pedestal effect". This is a spectral blue-shift which occurs in the background spectrum when sunlight is absorbed on a positive thermal anomaly. The shift makes it possible to detect smaller heat flow anomalies than would normally be detectable by NIMS. Thermal and heat flow measurements will be made by NIMS and PPR (Galileo's Photopolarimeter Radiometer), including the temperatures of Io's hot spots on the nightside and of cooling curves during eclipses of 10 by Jupiter.

The major scientific objectives for NIMS at Io are: (i) determining surface composition, temperatures, and heat flow; (ii) investigating atmospheric composition and (iii) determining timescales for different types of volcanic activity.

In terms of surface composition, NIMS will investigate the surface mineralogy and the temperatures of Io*s hot spots by making global and local maps in 102 to 408 wavelengths. Temperature variations and the distribution of SO_2, silicates, and other species will be mapped on a global scale at medium resolution (50-120 km/NIMS pixel) and on a local scale at high resolutions (5-25 km/NIMS pixel). The two-year tour will enable NIMS to identify temporal and latitudinal variations in the composition and temperature of surface features and plumes at all longitudes. NIMS will view parts of the north and south polar region (including the southern pole) during Jupiter orbit insertion, which will be an opportunity to search for unusual species cold-trapped in these regions.

To determine atmospheric composition, N] MS will perform limb scans to place limits on the atmospheric density of $S0_2$ and to investigate its source. In addition, NIMS will obtain temperatures of active plumes and search for compositional variations within and above them. Observations of Io's nightside will be made to search for auroral effects.

NIMS will monitor Io*s volcanic activity and search for volcanic outbursts throughout the

mission. The instrument will map the distribution and temperature variation of hot spots, including the very hot silicate sources (> 10CK)K) and the molten sulphur pods (400-600K). Measurements will be made on the dayside and nightside, and during eclipse. NIMS will monitor temporal changes in the global distribution of SO_2 and other species. Specific hot spots (Pele, Loki, and Kanehekili) will be targeted for more frequent monitoring, with time intervals between observations varying from minutes to months.

3.2 Icy **Satellites**

Current knowledge regarding the compositions of J upiter's icy satellites are described in detail by Calvin et al. (this issue). Recent observations include the following: the ubiquitous presence of water ice, the distinctive ultraviolet signature of SO_2 on Europa (e. g. No]] et al., this issue; Sack et al. 1992), the similarity of the spectral signature of Callisto's dark materials to high-iron clays (Calvin and Clark, 1991), the marked spectral difference between the dark material on Europa and that on Ganymede and Callisto, and the interesting new absorption feature discovered on the trailing hemisphere of Ganymede (Spencer et al., this issue).

Europa

Eur opa poses an ensemble of challenging scientific questions. These can be grouped around themes of global resurfacing, heat flow, composition, tectonophysics, and exogenic processes. Europa has been completely resurfaced and is part of an evolutionary sequence seen among the icy Galilean satellites. Apparently, neither Ganymede nor Callisto experienced such a complete global event.

The detection of only a few craters on Europa by the Voyager cameras sets a relatively young age for its surface. Did resurfacing occur as a discrete event, as a series of episodic processes, or as a long continuous process? Is this resurfacing active today? NIMS is uniquely capable of measuring the timeline of emplacement of different surface units by detecting small compositional changes in the surface ice. These small changes could indicate different source regions or perhaps different ages for the surface ices.

Clearly, a large amount of heat is involved in Europa's resurfacing. The source of this energy

is not understood. Models involving radio-nucleides, tidal interaction, and bombardment by asteroids, comets and other small bodies have thus far proved unsatisfactory. Compositional differences may give clues to the temperatures of melts that formed the surface. Setting limits on the heat flowing from the interior of Europa would provide an important constraint on models for resurfacing and internal structure. NIMS can search for small, relatively warm (≥ 180 K) anomalies at night. During the daytime the thermal pedestal effect may shift emission into the NIMS spectral range. Indirect indicators of thermal anomalies may also be present: "holes" in the surface distribution of volatile species and spatial changes in composition may indicate the presence of thermal anomalies.

The more volatile species will preferentially condense in the polar regions where the temperatures are coldest, thus scans of the polar regions may find species more volatile than water. A quantitative inventory of these species will help to identify interior compositions that have contributed to the form and shape of Europa's surface.

NIMS will be able to detect hydrated, some iron-baring minerals, and the presence of clathrates in or on Europa's relatively clean ice. The identification of particular compositions and the mapping of their spatial extent is fundamental to the recognition of distinct surface units. These will be characterized on local, regional, and global scales. The compositional boundaries and their relationships to tectonic features is particularly important for revealing the sequence of surface-forming events and thus the geologic history.

Europa is subject to a number of exogenic processes, of which cratering and implantation of magnetospheric species are the most prominent. NIMS can recognize large palimpsests discriminated by spectral variance. The composition of crater filling melts can be determined and will provide an indication of any differences in composition with depth.

The Jovian magnetosphere co-rotation velocity exceeds the orbital velocity of Europa, so magnetospheric ions are continually bombarding Europa's trailing hemisphere. Optical signatures of this effect are apparent in the ultraviolet, where at least two signatures are present. One signature, measured by the IUE satellite, mimics an UV SO_2 absorption band (Lane et al., 1981). The other,

seen by the Voyager cameras, is a general decrease of the UV albedo (Nelson et al., 1987). In both cases the signature is strongest at the center of the trailing hemisphere and weakest in the center of the leading hemisphere. In the Voyager data, the general intensity of the darkening follows a cos(z) relationship, where z is the angular distance on Europa's globe from the trailing point (Nelson et al., 1987). The SO_2 absorption band will be recognized by NIMS at 4.1 microns so that the distribution of this absorption can be mapped in detail.

Tectonic effects expected to be visible include the motion of crustal plates and resurfacing mechanics. A definite time sequence is evident in some of the offset relationships seen in the lineaments on Europa. Plate rotation is also evident. NIMS will contribute to the study of these features by adding compositional differences apparent in the infrared as a criterion for making distinctions.

From compositional and temporal relationships, NIMS data can establish whether or not the melts reaching the surface change with time. This can depend upon the number of melt reservoirs available and the fractionation of a reservoir as melt is withdrawn or erupted to the surface. For all of the resurfacing mechanisms that move melt to the surface (including crater flooding, fluence from lineaments, or more traditional aqueous floods in great sheets across the surface), NIMS infrared maps will provide the key to understanding the resurfacing of Europa.

Ganymede

Ganymede shows the greatest geologic diversity of the three icy satellites and displays analogues of processes evident on Europa and Callisto, as well as its own unique aspects. There is a fresh-appearing polar cap, a variety of crater forms (bright and dark rayed, dark floored, dark haloed, palimpsests), planet-wide sets of arcuate furrows as well as smaller grooved and ridged terrain, and apparent smooth, flooded basins [e.g. Shoemaker et al. 1982,]. Albedos of various terrains overlap with all but the darkest terrains on Callisto and the brightest on Europa [Johnson et al. 1983]. Schenk and McKinnon [1985] have recognized dark halo craters as evidence of dark terrain excavation, while dark ray and dark floor craters are inferred to be due to projectile contamination.

Spectral information on such widely diverse terrains can identify absorption features masked in the hemisphericall y-averaged observations obtainable from Earth. As a minimum, NIMS observations will yield important separation of ice and dark material spectra obscured by terrestrial atmospheric constituents. There are known leading/trailing hemisphere dichotomies on Ganymede; NIMS will be able to determine if these are driven by water ice grain size and purity, or by . fundamental differences in the mineralogy of the units. Subtle absorption features exist or are suggested on the trailing hemisphere [Spencer and Calvin, this issue; Calvin et al., this issue]. NIMS will search for confirmation of the infrared features or companions to the observed visible absorption feature. Examination of dark terrains will yield information on the mineralogy of impactors and excavated materials. Compositional information on the impactors is relevant to outstanding questions of whether the impactor populations for the outer planets are different from those for the terrestrial planets, It has been suggested that the deep interior of Ganymede might be exposed either in palimpsests or in central peak domes [Thomas and Squyres, 1990; Schcnk, 1993]. Characterization of these units by NIMS could reveal the composition of the mantle. Also, in relation to dark terrain, there is evidence for smooth resurfacing [e.g. Murchie et al. 1990] and the mineralogy of such units will have implications for the early thermal history of Ganymedc. Global compositional information for the dark material on Ganymede and its similarity or difference to that found on Callisto can provide clues to the diverging histories of these two, most similar, siblings. This comparison also provides information on the extent to which dark material has been excavated from the interior rather than emplaced by impacts (the inferred dominant source for dark material on Callisto).

Spectral observations of the polar shroud will give an indication of grain size and thickness of the deposit, thus yielding an estimate for the age, and can help constrain whether the cap is forming dynamically from sublimation or is an ancient remnant undergoing net erosion. Photometric and compositional information on the grooved and furrowed terrains may help constrain their mode of emplacement or formation.

NIMS will use limb scans to look for molecular oxygen airglow emissions from a possible

tenuous atmosphere on Ganymede. This experiment will be done in collaboration with Galileo's UVS (Ultraviolet Spectrometer).

Callisto

The Voyager encounters of 1979 provided new insight into Callisto's basic characteristics and gave us a look into Callisto's geologic past. Telescopic observations and laboratory measurements have significantly added to our knowledge of Callisto, but there. are still many unanswered questions.

Callisto appears to be the most primitive and unaltered of the Galilean satellites and has a relatively small number of terrain types. Major surface features include multi-ring structures with scarps and graben, palimpscsts, catenae, and a variety of craters. The.re are indications of multiple resurfacing processes, such as volcanism and cometary impact occurring on Callisto (e.g. Schenk and McKinnon 1994), but no evidence of the widespread resurfacing which occurred on Europa and Ganymede.

Spectral data providing the mineralogy and composition of Callisto's surface features will give insight into the extent and mechanisms of the resurfacing processes. Callisto's well-preserved surface places it in the unique position of providing an opportunity to study individual ancient processes, with material from features distinguishable from background surface material. The mineralogy will also aid in determining whether the resurfacing process is exogenic or endogenic in origin.

Non-icy components or dark materials cover as much as 60- 80% of Callisto's surface and have very low albedo. Unlike Ganymede and Europa, Callisto's non-ice component is a major contributor in hemispherically averaged ground-based spectra. Laboratory measurements indicate that a homogeneous mixture of ice, serpentinite, and magnetite provide the best comparison to telescopic spectra (e.g. Roush et al. 1990). Ground-based observations have revealed absorption features at 2.8, 2.9, and 3.4 microns, and potentially a 3.1 micron feature, which have been suggested to be ammoniated clays (Calvin and Clark, 1993).

NIMS observations of Callisto will clarify the composition, variability, and origin of both icy and non-icy materials residing on the. surface. In addition, hemispherical differences and the existence

of minor components with limited spatial distribution will be mapped. If subsurface material has been uplifted, as the Valhalla pal impsest and graben seem to suggest, the new compositional information could lead to an understanding of Callisto's formation and early geologic conditions.

4. SATELLITE OBSERVATIONAL PLANS

The NIMS observing plan for each of the Galilean satellites is described below. Planning is still underway and input from the community as well as new discoveries prior to Galileo's arrival at Jupiter may justify changes, particularly in the choice of wavelengths for specific observations. There will be a small amount of flexibility to make changes to the observing plans for the later orbits of the satellite tour based on results from Jupiter orbit insertion and from the early tour orbits. Many of the observations presented here have been coordinated with the other remote sensing instruments. This optimizes the science return by obtaining the maximum spatial and spectral coverage for targeted areas on the satellites,

4.110

The NIMS observing plan for Io can most easily be described by separating those observations obtained during Jupiter orbit insertion (when the spacecraft makes its only close flyby of Io) from those observations obtained during the rest of the satellite tour (global observations having wide longitudinal and good temporal coverage but limited spatial resolution). These two sets of observations will complement one another and should greatly enhance our present knowledge of Io's mineralogy, atmospheric composition, and volcanic activity.

4.1.1. **Jupiter Orbit Insertion**

The best opportunities for observing 10 will occur when the spacecraft flies by Io at an altitude of 1,000 km on December 7, 1995. NIMS will make ten close-range observations of Io during Jupiter Orbit Insertion (Figure 6 and Table 2a). Their objectives are:

(i) Obtain global coverage at the maximum feasible spectral and spatial resolutions. Observations HRSPEC and GLOBAL are spectral maps of 10's dayside, with the first obtaining high spectral resolution (50 % 408 and 50% 204 wavelengths) at spatial resolutions of about 50 km/NIMS

pixel, and the second obtaining high spatial resolution (about 25 km/NIMS pixel) at modest spectral coverage (17 wavelengths).

(ii) Obtain high spatial resolution samples of selected areas at high spatial resolution (a few km per NIMS pixel) and good spectral resolutions (102 to 204 wavelengths): NIMS will take advantage of the spacecraft's close pass by Io to sample a variety of terrain types. The Prometheus and Maui region observation (HRCHEM) includes samples of dark and light terrains shown in Voyager images. A higher spatial resolution observation of the persistent Prometheus vent (PROMVT) will be made at a closer range to sample the vent area and plume in more detail. Other targets include the mountain and mesa region on the northwestern edge of Colchis Regio (MTMESA), the Volund vent area, a hot spot observed by the Voyager IRIS instrument (VOLU ND), and the Colchis lava flow region (COLCHS).

(iii) Map part of Io's nightside and the Loki plume using the NIMS thermal channels, together with Galileo's Photopolarimeter Radiometer (PPR). Observation HOTSPT maps the Kanehekili hot spot region. Observation LOKI PL consists of three limb scans from the surface to about 200 km altitude to characterize the plume's temperature distribution.

(iv) Detect atmospheric SO_2 by means of limbscans at high spatial resolution (about 8 km/NIMS pixel). The three limbscans in observation LBSCAN each cover about 270 km (with about 200 km being above the surface) at 2 wavelengths, with one wavelength centered on the strong SO_2 band at 4.1 microns and the other sampling the continuum. One of the scans is near the potentially active Amarani-Maui region, while the other two avoid known active areas.

4.1.2. Satellite Tour

Following Jupiter orbit insertion, NIMS makes about 100 global observations of Io during the two-year Jupiter tour at spatial resolutions ranging from about 100 to 1000 km/pixel (Figure 6, Table 2b). These observations focus on monitoring global temporal changes of surface composition (such as SO_2 frost distribution) and temperature, using between 102 and 408 wavelengths. Observations of both the dayside (CHEMIS) and nightside (THRMAL) are made, covering most longitudes at least

once during each orbit. As shown in Figure 6, Io's closest approach in several orbits is used to map the dayside at high spectral resolution (HRSPEC). One high spectral resolution observation of the nightside disk (NSPEC) is made during the G 1 orbit to search for auroral effects and to investigate the source of fluorescence.

Jo will be observed approximately every 4 hours within +/- 48 hours of Io closest approach in each orbit. Intervals between Io closest approach in consecutive orbits range from about 1 to 3 months. Additional monitoring observations (VOLCAN) target selected hot spots (mainly Pele, Kanehekili, and Loki). These observations will be obtained at time intervals varying from minutes to days and at spatial resolution ranging from 120 to 700 km/NIMS pixel.

Eclipses of Io by Jupiter will be observed as Io enters Jupiter's shadow (COOLCV) and again as Io emerges from eclipse (WARMCV).

4.2 **Europa**

Fourteen NIMS observations of Europa are planned, covering most of the longitudes of the satellite. A few gaps in longitude coverage exist due to the practical limits on the geometry of the spacecraft orbits. Each orbit in the tour presents unique phase angle or longitude coverage. Jupiter orbit insertion and orbit El 1 give excellent polar passes. The planned NIMS observations of Europa are summarized in Figure 7 and Table 3 for each of the orbits of the Galileo tour. These observations have been divided into three categories: polar observations, global observations, and high resolution spectral observations.

Two main polar observations, SOPOLE and NOPOLE, are planned for Europa. The Jupiter orbit insertion period provides the only opportunity to observe Europa's south polar region. This observation covers the lit portion from the pole up to approximately 60" S latitude at resolutions of 16 to 20 km/NIMS pixel in 204 wavelengths. The best opportunity to observe Europa's north polar region occurs during orbit El 1 at spatial resolutions as high as 0.5 km/NIMS pixel and phase angles ranging from approximately 90" to 67°. The north pole observations are acquired with 102 wavelengths except for a strip within the mosaic that is done at 204 wavelengths. This strip will be used to search

for compositional differences between the south and north poles. The polar observations during Jupiter orbit insertion and E11 present good opportunities for N I MS to detect frozen species more volatile than water.

The other nine orbits in the tour provide views of a variety of different terrains at a wide range of phase angles (from 27° to 147", see Figure 6). NIMS spatial resolution at periapsis for these encounters ranges from 300 m in orbit E6 to 92 km in orbit G1. The spatial resolution of these observations is reduced somewhat from the highest possible to maximize longitudinal coverage.

Global coverage includes all longitudes except 0° to 90° at spatial resolutions of 90 km/NIMS pixel or better. The global observations (PHINEA, LINEA) cover longitudes of 21O" to 1500 and 300° to 340", respectively. ASTER] (in orbit E4) and TINC1 (in orbit E6) will present a particularly good data set from which to study the composition and tectonic differences between the leading and trailing hemispheres of Europa. FLEXUS and ADONIS are complementary global observations that provide longitude coverage from 220° to 100" (on the trailing hemisphere).

The high spectral, high spatial resolution observations are performed at 408 wavelengths (SUCOMP 1,2, and TYREMA). The high data volume of these observations restricts the total number of observations to six (Fig. 6). SUCOMP 1 and 2 observe a high and a low albedo terrain, respectively, to assess the relationship of albedo difference to composition. These observations obtain high spatial resolution (1- 10 km/NIMS pixel) samples of specific areas on Europa, such as Tyre Macula, which will be observed by all of Galileo's remote sensing instruments,

A limb observation (ELIMB) is planned to search for evidence of the existence of an atmosphere or volcanic plumes.

4.3 Ganymede

In keeping with the general satellite science objectives, we have planned 30 observations of Ganymede (Table 4) to obtain global mapping at high spectral resolution, and selected targets at high spatial and high spectral resolution. Figure 8 shows the areas covered by these observations, which are obtained during five orbits (GI, G2, G7, G8, and C9). With the exception of the atmospheric limb

scan and two spectral end member targets, all observations are obtained in 204 wavelengths. Using global observations, NIMS will map about 90% of the surface at spatial resolutions of approximately 100 km/NIMS pixel. The remaining 10% is unobservable due to geometry and spacecraft constraints. The unobserved region is concentrated in the longitude range 10 to 40 degrees.

Two regional observations of the north and south poles are planned (observations SRPOLE and NRPOLE, see Table 4). The south polar region is observed in the first orbit from longitudes 120 to 240 and latitudes from -55 to -90 degrees, with spatial resolution of about 35 km/NIMS pixel. The north polar region is observed in the second orbit, covering the longitude range 150 to 240 degrees, and the latitude range 60 to 90 degrees, the spatial resolution being about 9 km/NIMS pixel.

Observations of dark terrains include the Galileo Regio area around Memphis Facula (MEMPIS) which is acquired with a spatial resolution of about 42 km/NIMS pixel. Two observations (LIDARK and DARTRL) are planned in the Marius Regio area (on the trailing side), with spatial resolutions of about 3 and 11 km/NIMS pixel respectively. Observation DARTRL will return 408 wavelengths to search for possible narrow spectral features. On the leading hemisphere we have planned one observation (DARLED) which has spatial resolution of about 15 km/NIMS pixel.

Similarly, several targeted observations of bright terrains are planned to determine spectral end members and to search for variability among specific terrains on the leading and trailing hemispheres. One observation (BRILED) of the leading hemisphere is planned near the equator at 68 degrees longitude using 408 wavelengths. The second observation (BRITRL) is on the trailing hemisphere in the Sippar Sulcus area. Spatial resolution is about 20 and 9 km/NIMS pixel, respectively. A third observation (BRFRGR) is planned over the north pole and across the boundary of the polar hood, at a spatial resolution of about 2 km/NIMS pixel.

Given their areal dominance, we have planned a number of observations of grooved and furrowed terrains, which include the terrains near Memphis Facula (MEMPIS) with a spatial resolution o about 42 km/NIMS pixel, the terrains surrounding the craters Osiris (OSIRIS) and AmOn (AMUN) at resolutions of about 40 and 20 km/NIMS pixel respectivel y, and the large sulci Nippur Sulcus

(NIPPUR, TRANSI), Sippar Sulcus (SIPPAR), and Uruk Sulcus (URUK) at resolutions ranging from about 9 to 19 km/NIMS pixel.

Observations of a variety of crater forms are also planned (Table 4). These include bright rayed, dark rayed, dark haloed and dark floored craters, as well as a central dome crater and palimpsests. Some specific craters to be observed include Edfu Facula (EDFU), Punt Facula (PUNTFA), the Gilgamesh palimpsest (GILMES), the central domed crater Eshmun (ESHMUN), the bright rayed crater Tammuz (TAMMUZ), the dark rayed craters Mir (MIRRAY), Antum (ANTUN), Kitt (KITTU), Isis, and Ptah (ISPTAH). Spatial resolutions vary depending on crater size and viewing geometry and range from about 4 to 40 km/NIMS pixel.

A limb scan observation (LIMB) is planned to search for an atmosphere around Ganymede. This observation has a spatial resolution of approximately 5 km/NIMS pixel and a small number of wavelengths (less than 8).

5.4 Callisto

Throughout Galileo's two year tour, NIMS will observe Callisto in six of the eleven orbits including three close encounters. The observations are designed in keeping with the overall NIMS science theme for Callisto: composition, composition, and composition. The observation plan is summarized in Table 5 and Figure 9.

Global context maps at 204 wavelength spectral resolution are taken in each of the 6 orbits. The spatial resolution and surface coverage vary according to geometry and downlink resources available, but the typical resolution lies between 100 and 200 km/NIMS pixel. These observations include both leading and trailing sides and provide a base map of global surface spectra. Regional observations at 102 and 204 wavelengths are taken on four orbits, with spatial resolutions ranging from 20 to 50 km/NIMS pixel. The areas chosen are regions of particular interest such as the Asgard and Valhalla multi-ring structures, the south pole, and high northern latitudes.

"Postage-stamp" observations (high spatial resolution, small areal coverage) and spectroscopic scans of 204 and 408 wavelengths are obtained on four 4 orbits and constitute the remaining set of

Callisto observations. The spatial resolution varies from 1 to 20 km. The observations are taken at the best spatial resolution obtainable.

Postage-stamp observations and spectroscopy scans are nested within the regional observations and the regional observations are nested within the global observations, hence providing an integrated NIMS Callisto data set.

5. SUMMARY

The currently planned observations for the Near Infrared Mapping Spectrometer experiment on the Galileo spacecraft consist of global observations at high spectral resolution which provide context for a small number of high spatial, high spectral resolution observations of specific areas of interest. A limited number of these special interest observations can be returned, so the choice of targets is of great importance to the planetary science community. We expect that alternate choices of targets will be proposed by researchers outside the Galileo Project prior to the end of the planning phase for the spacecraft sequences. Selection of specific targets is difficult because the Galilean satellites have not previously been mapped in this wavelength region at spatial resolutions greater than about 4 pixels/hemisphere. It is both reasonable and exciting to contemplate that this new dataset will greatly expand our understanding of the Galilean satellites.

ACKNOWLEDGEMENTS: The work reported herein was supported by the Galileo Project and was performed at the Jet Propulsion Laboratory under contract with the National Aeronautics and Space Administration.

FIGURE CAPTIONS

FIGURE 1: Schematic diagram of the NIMS instrument and scanning motions. The instrument is shown as it would appear sitting on the spacecraft scan platform. The cone angle motion of the scan platform is illustrated by the large arrows. The internal 20-position spatial scan, produced by motion of the telescope secondary mirror, is in the orthogonal cross-cone direction. The position of the initial pixel in a major frame (RIM) is shown as pixel 1. The plane of spectral dispersion is parallel to the plane of cone angle motion. (After Carlson et al. 1992).

FIGURE 2: Radiance values for the NIMS instrument, The sensitivities of the first 14 detector channels are set for full scale (data number = 1023) for a radiance about 20% greater than that of a normally illuminated Lambertian surface at the orbit of Jupiter. The measured saturation radiances are shown for each detector along with their intrinsic noise levels and estimates of the induced noise from the magnetosphere at the orbit of Io. The radiance for a solar illuminated Lambertian surface is denoted by the solid curve ($\mu_0 p = 1$) and, just below it, the dashed curve approximates the Io reflectance spectrum. Blackbody radiances are also indicated for various temperatures.

FIGURE 3: Two examples of NIMS spectra obtained during Galileo flybys. (3a): Nightside spectra of Venus (Carl son et al. 1991), illustrating the spectral resolution. (3 b): NIMS and ground-based spectra of 243 Ida. The ground-based observations, offset by 0.02, are by Tholen (pers. comm. 1993) and Binzel et al. (1993). Considering the differences in calibration methods (laboratory vs. standard stars) the agreement is excellent.

FIGURE 4: Satellite Tour 92,-14A Petal Plot: orbits dui ing Galileo's tour of Jupiter viewed from above the ecliptic plane. The individual orbits are numbered. The orbits have a mean spacing of 40 days. The time from Jupiter orbit insertion to first encounter is approximately 6 months. Details of

the individual orbits are given in Table

FIGURE 5: Reflectance of some minerals and frosts at the NIMS spectral resolution. The minerals (3a) are combined from the libraries of Clark et al. [1993] and Salisbury et al. [1991], with offsets of 0.35 (Gypsum) and 0.6 (Dolomite). The frosts (3b) are from Fink and Sill [1982], with offsets of 0.5 (H_2S), 1.2 (NH_4HS), and 1.75 (NH_3).

FIGURE 6: Coverage map of planned NIMS observations of Io. The observations plotted on the map are the high spatial resolution observations planned during Jupiter orbit insertion. The numbers on the map correspond to the observations described in Table 2a. The lower graph shows the global coverage of Io planned for the rest of the tour. Spatial resolution is shown in parentheses (in km/NIMS pixel). The color code represents the number of wavelengths returned (Blue = 408, Green = 204, Orange = 102, Red = 51, Brown = < 51). The dashed lines represent dayside coverage, the solid lines are nightside coverage. The eorresponding orbit designations are shown on the left.

FIGURE 7: Coverage map of planned NIMS observations of Europa. Higher spatial resolution observations are plotted on the map; global coverage is plotted on the bar graph underneath. The numbers on the map and below the graph bars correspond to the observations described in Table 3. NIMS spatial resolution is shown in parentheses for the global observations (in km/NIMS pixel). The color code represents the number of wavelengths returned (Blue = 408, Green = 204, Orange = 102, Red = 51, Brown = < 51).

FIGURE 8: Coverage map of planned NIMS observations of Ganymede. Higher spatial resolution observations are plotted on the map; global coverage is plotted on the bar graph underneath. The numbers on the map and below the graph bars em-respond to the observations described in Table 4. NIMS spatial resolution is shown in parentheses for the global observations (in km/NIMS pixel). The

TABLE 1: Summary of Galileo's satellite tour. The encounters designated with N are non-targeted but reasonably close encounters which provide opportunity to obtain additional longitude coverage or phase angle information for the designated satellites. The observing time available at altitudes less than **5,000** km is very limited.

TABLE 2a: Io observations during Jupiter orbit insertion. These are the highest spatial resolution observations of **Io** during the mission. Numbers in the first column correspond to numbers on the map in Figure 5.

TABLE **2b: Io** observations during the satellite tour. The coverage and spatial resolution of observations NSPEC, HRSPEC, CHEMIS, and THRMA1. are shown in Figure 5.

TABLE 3: NIMS Europa observations: the numbers in the second column correspond to the numbers in Figure 6.

TABLE 4: NIMS Ganymede observations: the numbers in the second column correspond to the numbers in Figure 7.

TABLE 5: NIMS Callisto observations: the numbers in the second column correspond to the numbers in Figure 8.

REFERENCES

Binzel, R. P., Xu, S., and Bus, S. J.: Spectral variations within the Koronis family: Possible implications for the surface colors of asteroid 243 Ida. Icarus, 608-611, 1993.

Blaney, D. L.; Johnson, T. V.; Matson, D. L.; and Veeder, G. J.: Volcanic eruptions on Io: Heat flow, resurfacing, and lava composition. Submitted to nature, 1994.

Broadfoot, A.I.., M.J.S. Belton, P.Z. Tackas, et al.: Extreme ultraviolet observations from the Voyager encounter with Jupiter. Science, 204, 979-82., 1979.

Calvin, W. M., and R.N. Clark, Spectral distinctions between the leading and trailing hemispheres of Callisto: New observation. Icarus, 104, 69-78, 1993.

Calvin, W. M., Clark, R. N., Brown, R. H., and Spencer, J. R., Spectra of the icy Galilean satellites from 0.2 to 5 microns: A compilation, new observations, and a recent summary. J. Geophys. Res., this issue.

CarlSon, R. W., Weissman, P. R., Smythe, W. D., Mahoney, J. C., and the NIMS science and engineering team: Near-Infrared Mapping Spectrometer experiment on Galileo. Space Science Reviews, 60, 457-502, 1992.

Clark, R. N., G.A. Swayze, T.V.V. King, A. Gallagher, and W.M. Calvin, The U.S. Geological Survey Digital Spectral Library: Version 1:0.2. to 3.0 microns. U. S.G.S. Open File Report 93-592, 1993.

Clew, G.D. and M.H. Carr: Stability of sulfur slopes on Jo. Icarus, 44, 268-79, 1980.

Fanale, F. P., R.H. Brown, D.P. Cruikshank, and R.N. Clark, Significant absorption features in 10's IR reflectance spectrum, Nature, 280, 761-763, 1979.

Fanale, F. P., W. Banerdt, 1.,. Elson, T.V. Johnson, and R. Zurek. In: Satellites of Jupiter (D. Morrison, Ed.), pp. 756-781, University of Arizona Press, Tucson, U. S. A., 1982.

Fink, U., and G.T. Sill, The infrared spectral properties of frozen volatiles, In: Comets (L.L. Wilkening, Ed.), pp. 164-202, University of Arizona Press, Tucson, 1982.

Goguen, J. D., Sinton, W. M., Matson, D.I.., R.R. Howell, H.M. Dyck, T.V. Johnson, R.H.

Brown, G.J. Veeder, A. I.. Lane, R.M. Nelson, R.A. Mclaren: Io hot spots: infrared photometry of satellite occultations. Icarus 76, 465-84, 1988.

Gradie, J., and J. Moses: Spectral reflectance of unquenched sulfur. Lunar and Planetary Science Conference, 14, 255-6, 1983.

Greenberg, R., Time-varying orbits and tidal heating of the Galilean satellites. In: Time-variable Phenomena in the Jovian System, ed. by M.J. S. Belton, R.A. West and J. Rahe, pp. 100-115, NASA SP-494, Washington, D. C., 1989.

Johnson, T. V., D. Morrison, D.L. Matson, G.J. Veeder, R.H. Brown, R.M. Nelson: Volcanic hotspots on Io: stability and longitudinal distribution. Science, 226, 134-7, 1984.

Johnson, T. V., G.J. Veeder, D.L. Matson, R.H. Brown, R.M. Nelson, D. Morrison: Io: evidence for silicate volcanism in 1986. Science, 242, 1280-3, 1988.

Johnson, T. V., L.A. Soderblom, J.A. Mosher, G.E. Danielson, A.F. Cook, and P. Kupperman, Global multispectral mosaics of the icy Galilean satellites, J. Geophys. Res., 88, 5789-5805, 1983.

Hanel, R. A., B. Conrath, M. Flasar, et al.: Infrared observations of the Jovian system from Voyager 1. Science 204, 972-976, 1979.

Hapke, B.: The surface of Io: a new model. Icarus, 79, 56-74, 1989.

Howell, R. R., D.P. Cruikshank, and F.P. Fanale. Sulfur dioxide on Io: Spatial distribution and physical state. Icarus, 57, 53-92, 1984.

Khanna, R. K., M.J. Ospina, and J .C. Pearl. Surface composition of Io: Analysis of the thermal emission spectrum in the light of laboratory data. In: Jo, an International Conference, San Juan Capistrano Research Institute, pp. 54, 1993.

Kumar, S.: The stability of an SO_2 atmosphere on Io. Nature, 280, 758-760, 1979.

Lane, A. L., R.M. Nelson, D.L. Matson, Evidence for sulphur implantation in Europa's UV absorption data. Nature, 292, 38-39, 1981.

Lellouch, E., M. Belton, 1. de Pater, G. Paubert, S. Gaulkis, and "I'. Encrenaz: The structure,

stability, and global distribution of Io's atmosphere. Icarus, 98, 271-295, 1992.

Matson, D. L.; G.A. Randsford; T.V. Johnson. J. Geophys. Res., 86, 1664-1672, 1981.

Matson, D. L.; T.V. Johnson; D.L. Blaney; and G.J. Veeder: Ground-based observations of Io. Submitted to IUGG Quadrennial Report, 1994.

McGrath, M. and R.E. Johnson: Magnetospheric plasma sputtering on Io's atmosphere. Icarus, 69, 519-531, 1987.

Moore, J. M., A.S. McEwen, E.F. Albin, R. Greeley. Topographic evidence for shield volcanism on Io. Icarus, 67, 181-183, 1986,

Morabito, L. A., S.P. Synnot, P.N. Kupferman, S.A. Collins: Discovery of currently active extra-terrestrial volcanism. Science, 204, 972, 1979.

Murchie, S. L., J.W. Head, and J.B. Plescia, Tectonic and volcanic evolution of dark terrain and its implications for the internal structure of Ganymede, J. Geophys. Rcs., 95, pp. 10, 743-10,768, 1990.

Nash, D. B.: Sulfur in vacuum: Sublimation effects on frozen melts and applications to Io*s surface and torus. Icarus, 72, 1-34, 1987.

Nash, D. B. and R.M. Nelson, Spectral evidence for sublimates and adsorbates on Io, Nature, 280, 763-766, 1979.

Nash, D.B. and R.R. Howell. Hydrogen sulfide: evidence from telescopic and laboratory infrared spectra. Science 244, 454-457, 1989.

Nash, D. B., A case for Na_2S on Io's surface: Sulfide volcanism?, San Juan Capistrano Research Institute International Conference on Io, 75-76, June, 1993.

Nelson, R. M., A.L. Lane, D.L. Matson, F.P. Fanale, D.B. Nash, T.V. Johnson: Io: Longitudinal distribution of S02 frost. Science, 210, 784-6, 1980.

Nelson, R. M., A.L. Lane, D.L. Matson, B.J. Buratti, E.F. Tedesco, Spectral geometric albedo of the Galilean satellites from 0.24 to 0.34 microns: observations with IUE. Icarus, 72, 358-380, 1987.

Noll, K. S., H.A. Weaver, and A. M. Gonella, The albedo spectrum of Europa from 2200 A to 3300 A. J. Geophys. Res., this issue.

Pearl, J., R. Hanel, V, Kunde et al . : Identification of gaseous SO_2 and new upper limits for other gases on Io. Nature, 280, 755-8, 1979.

Pieri, D. C., S.M. Baloga, R.M. Nelson, C. Sagan: Sulphur flows at Ra Patera, Io. Icarus, 60, 685-700.

Roush, T. L., J.B. Pollack, F.C. Witteborn, J. Il. Bregman, and J.P. Simpson: Ice and minerals on Callisto: A reassessment of the reflectance spectra, Icarus, 86, 3S5-382, 1990.

Sack, N. J., R.E. Johnson, J. W. Boring, and R.A. Baragiola, The effect of magnetospheric ion bombardment on the reflectance of Europa's surface, Icarus, 100, 534-540, 1992.

Sagan, C.: Sulphur flows on Io. Nature, 280, 7503, 1979.

Salama, F., L.J. Allamandola, F.C. Witteborn, D.P. Cruikshank, S.A. Sandford, and J.D. Bregman, The 2.5-5.0 micron spectra of Io: evidence for H_2S and H_2O frozen in $S0_2$, Icarus, 83, 66-82, 1990.

Salisbury, J. W., L.S. Walter, N. Verge, and D.M. D'Aria, Infrared (2. 1-25 microns) Spectra of Minerals, John Hopkins University Press, 1991.

Schcnk, P. M., and W.B. McKinnon, Dark halo craters and the thickness of the grooved terrain on Ganymede, Proc. Lunar Planet. Sci. Conf. 16, in J. Geophys. Res. Supp. 90, C775-C783, 1985.

Schenk, P. M., and W.B. McKinnon, Callisto, entry for the Van Nostrand Reinhold Encyclopedia of Planetary Sciences, 1994, in press.

Schenk, P. M., Central peak and dome craters: Exposing the interiors of Ganymede and Callisto, J. Geophys. Res., 98, pp. 7475-7498, 1993.

Shoemaker, E. M., B.K. Luchitta, D. E. Wilhelms, J.B. Plescia, S.W. Squyres, The Geology of Ganymede, In: Satellites of Jupiter (D. Morrison, Ed.), pp. 435-520, University of Arizona Press, Tucson, 1982.

Smith, B. A., L.A. Soderblom, R. Beebe: The Galilean satellites and Jupiter: Voyager 2

imaging science results. Science, 206, 927-50, 1979.

Smythe, W. D., R.M. Nelson, and D.B. Nash, Spectral evidence for the SO_2 frost or adsorbate on Io's surface, Nature, 280, 766-767, 1979.

Spencer, J. R., and W.M. Calvin, CCD spectra of the Galilean satellites: J. Geophys. Res., this issue.

Spencer, J. R., Calvin, W. M., and Person, M. J., CCD spectra of the Galilean satellites: Molecular oxygen on Ganymede. J. Geophys. Res., this issue.

Thomas, P. J., and Squyres, S. W., Formation of crater palimpsestson Ganymede, J. Geophys. Res., 95, pp. 19,161-19,174, 1990.

Veeder, G. J.; Matson, D. L.; Johnson, T. V.; Blancy, D. L., and Goguen, J. D.: Io's heat flow from infrared radiometry: 1983-1993. Journal of Geophysical Research, in press.

Wamsteker, W., R.L. Kroes, J.A. Fountain: On the surface composition of Io. Icarus, 23,417-424, 1974.

Wolf, A. A., and D.V. Bymes, Design of the Galileo Satellite Tour, AAS/AIAA Astrodynamics Specialist Conference, Victoria, B. C., August 1993.

Young, A. T.: No sulphur flows on Io. Icarus, 58, 197-226, 1984.

Table / Satellite Tour 92-14A Summary

Encounter	Satellite	Date	Inbound / Outbound	Altitude	Latitude	Objective
G1	Ganymede	4-M-96	In	500	24	Wake, Alfven Wing, UVS, gravity, reduce period
G2	Ganymede	6-Sep-96	In	200.	84	Alfven Wing, gravity, reduce inclination
C3	Callisto	4-Nov-96	In	1,096	15	Wake, Alfven Wing. UVS counter-rotate, Jupiter Occ.
E3N	Europa	6-Nov-96	out	31,800	0	Coverage (232" W. brig., Phase = 34°)
E4	Europa	19-Dec-96	out	895	1	Wake, Europa Occ., Jupiter Occ.
E5N	Europe	20-Jan-97	out	27,800	0	Occurs during solar conjunction interval
E6	Europa	20-Feb-97	In	589	-4	Europa Occ., Jupiter Occ., 10 Occ.
E7N	Europa	4-Apr-97	In	25.000.	-1	Coverage (133" W. Long., Phase = 52°), distant wake
G7	Ganymede	5-Apr-97	out	3,105	68	Alfven Wing
C8N	Callisto	6-May-97	In	33,200	-40	Coverage (72° W. Long., Phase = 43°)
G8	Ganymede	7 * 9 7	In	1,602	28	Ganymede Occ., Jupiter Occ., distant UVS
C9	Callisto	25-Jun-97	In	420	1	Callisto 000., Jupiter Occ., tail petal
G9N	Ganymede	26-Jun-97	in	80,200	1	Coverage (98" W. Long., Phase = 20°), distant wake
Clo	Callisto	17-Sep-97	In	528	6	Wake, Alfven Wing, Jupiter Occ., Rotate, UVS reduce period
E n	Europa	6-Nov-97	In	1,127	88	Alfven Wing

TABLE 2a
NIMS IO OBSERVATIONS DURING JUPITER ORBIT INSERTION

OBS NUMBER	ACTIVITY NAME	#λS	DESCRIPTION	RESOLUTION (km/NIMS pixel)	PHASE ANGLE (deg)	INCIDENCE ANGLE (deg)	EMISSION ANGLE (deg)
1	HRSPEC	408 AND 204	GLOBAL MAP OF IO'S DAYSIDE AT HIGH SPECTRAL RESOLUTION (50% AT 408 λS, 50% AT 204 λS)	~60	14°	11° to 103°	8° to 90°
2	GLOBAL	17	GLOBAL MAP OF IO'S DAYSIDE AT HIGH SPATIAL RESOLUTION	~25	15°	10° to 100°	6° to 90°
3	HRCHEM	82	HIGH SPATIAL RESOLUTION MAP OF PROMETHEUS AND MAUI REGIONS	~15	10°	8° to 59°	21° to 74°
4	M M	0	...RY HIGH SPATIAL RESOLUTION OBSERVATION OF MOUNTAIN/MESA REGION	~8	8	62°	63°
5	LIMBSCAN	2	LIMB SCANS TO DETECT SO2	~6	6°	62° to 79°	73° to 93°
6	PROMVT	204	VERY HIGH SPATIAL RESOLUTION OBSERVATION OF PROMETHEUS VENT	~5	6°	24°	28°
7	VOLUND	204	VERY HIGH SPATIAL RESOLUTION OBSERVATION OF VOLUND VENT	~3	8°	25°	
8	COLCHS	204	VERY HIGH SPATIAL RESOLUTION OBSERVATION OF COLCHIS AREA	~2	15°	13°	33°
9	HOTSPT	17	DARKSIDE THERMAL MAP OF KANEHEKILI REGION	~4	148°	134°	23°
10	LOKIPL	7	LIMB SCAN OF LOKI PLUME AND THERMAL MAP OF LOKI EVENT	~8	156°	113° to 139°	66° to 92°

TABLE 26

IO OBSERVATIONS DURING SATELLITE TOUR

NAME	DESCRIPTION	WAVELENGTHS	RESOLUTION RANGE (km)	ORBITS
NSPEC	High spectral, nightside, global	408	370	G1
HRSPEC	High spectral, dayside, global	408	120-300	G2,C3,E4 E4 , E6 C9,C10
CHEMIS	dayside, global	102	140-730	all
THRMAL	nightside, global	10?	"120-900	all
VOLCAN	monitoring of specific hot spots	12	140-930	all

TABLE 3

EUROPA

ORBIT	Number	Observation	Description	Spatial Resolution(km)	Phase Angle (deg)	Cone Angle (deg)	Incident Angle (deg)	Emission Angle (deg)	Wavelength
JA	1	SOPOLE	south pole long 240'-60'	17	85	95	64-92	8-56	204
G1	2	NHILAT	Northern Lat at long 180'-310'	92	28	151	36-114	26-90	102
C3	3	PHINEA	Phineus Linea	65	43	146	44-91	33-84	102
	4	LINEA	Lines terrain	16	34	137	49-114	36-90	102
	5	ELIMB	Limb observation	27	86	83	13-92	6-90	102
E4	6	SUCOMP1	surface composition, long 310'-320', light terrain	1.2	87	97	48	52	408
	7	SUCOMP2	Surface composition long 300°-310', dark terrain	4.3	66	118	48	53	408
	8	ASTERI	Asteri region	57	55	128	75	90	102
E6	9	TINC1	Trailing sick (long 160°-240°)	55	35	140	21-89	19-90	102
G7	10	FLEXUS	Flexus region	79	26	145	21-84	22-90	102
	11	TYREMA	Tyre Maeula	12.5	52	134	36-66	29-56	408
E11	12	TINC2	Leading side (long. 230°-240")	50	67	123	72-92	17-70	102
	13	ADONIS	Adonis linea	40	111	57	44-%	25-70	102
	14	NO POLE	North Pok (long 250°-200°)	0.56	67	109	59-106	0-40	204/102

TABLE 4

Ganymede

Observations	Observation Descriptions	Spatial Resolution (km)	Phase Angle (deg)	Incident Angle (deg)	Emission Angle (deg)	Number of Wavelengths
1 GLOBAL	Global map (longitude 190 to 240)	114	30	80	70	204
2 MEMPIS	Memphis Facula (palimpsest and furrows)	42	30	30	55	204
3 SRPOLE	South Pole region	36	29	84	76	204
4 GILMES	Gilgamesh (palimpsest with ring basin)	25	29	72	80	204
5 AMON	Amon, bright rayed crater in groove terrain	20	26	63	54	204
6 ISPTAH	Isis & Ptah, rayed craters on North Pole	17	25	72	66	204
7 NIPPUR	Nippur Sulcus (furrows, dark and groove terrain)	12	26	32	40	204
8 SIPPAR	Sippar Sulcus (dark and smooth groove terrain)	9	24	18	14	204
9 PUNTFA	Punt Facula (palimpsest with ring basin)	8	13	76	65	204
10 MIRRAY	Mir, a dark rayed crater	6	8	64	55	204
11 TAMMUZ	Tammuz, bright rayed crates	13	26	73	48	204
12 NRPOLE	North Pole region	9	30	79	81	204
13 ANTUM	Antum, dark rayed crater	4	24	59	37	204
14 BRFRGR	Bright frost terrain on North Pole region	2	23	83	79	204
15 GLOBAL	Global map (longitude 260 to 12)	107	62	5s	48	204
16 BRITRL	Bright ten-sin in trailing hemisphere	9	80	25	85	204
17 KITTU	Kittu, dark rayed crater	5	91	40	57	204
18 GLOBAL	Global map (longitude 230 to 270)	111	120	60	65	204
19 ESHMUN	Eshmun (central dome crater) and bright terrain	24	64	67	20	204
20 URUK	Uruk Sulcus (craters, furrows and groove terrain) "	19	68	27	54	204
21 TRANSI	Transition dark Marius Regio to bright Nippur Sulcus	15	66	80	47	204
22 LIDARK	Light dark material in Marius Regio	11	70	66	6	204
23 EDFU	Edfu Facula (dark floor crater and palimpsest)	7	82	39	59	204
24 LIMB	Limb scan for atmosphere (Not shown at map)	5	94	13	82	8
25 DARTRL	Very dark terrain (Marius Region) m trailing hemisphere	3	98	84	35	408
26 DARLED	Dark terrain m leading hemisphere	15	127	39	92	204
27 BRILED	Bright terrain m leading hemisphere	20	126	35	91	408
28 GLOBAL	Global map (longitude 60 to 200)	85	42	65	50	204
29 OSIRIS	Osiris, a central dome crater	41	19	89	70	204
30 GLOBAL	Global map (longitude 37 to 65)	82	81	81	37	204

TABLE 5

CALLISTO

Orbit	Observation Number and Name	Description	Spatial Resolution (km)	Phase Angle (deg)	Incident Angle (deg)	Emission Angle (deg)	Number of Wavelengths
G1	1 GLOBAL	Global context map (longitude 305 to 35)	955	75	13	90	204
G2	2 GLOBAL	Global context map (longitude 255 to 355)	211	62	35	90	204
C3	3 GLOBAL	Global context map (longitude 85 to 205)	120	51	116	90	204
	4 ASGARD	Asgard ring structure	20	50	43	17	102
	5 RINGS	Asgard ring traverse	10	45	50	26	204
	6 CRATER	Burr-a central pit crater	3	27	42	46	204
G8	7 GLOBAL	Global context map (longitude 60 to 175)	110	61	101	77	204
	8 SPOLE	South polar region	20	43	92	49	102
	9 BURI	Buri-bright rim crater	16	42	56	25	204
	10 ADLINDA	Adlinda region	16	51	72	20	102
	11 GLOBAL	Global context map (longitude O to 90)	100	85	93	57	204
C9	.12 SKULD	Crater within Valhalla ring structure	0.8	130	47	69	204
	13 ANARR	Anarr-bright rim crater	2	118	80	65	204
	14 NOLAT	North latitude region	27	93	91	70	102
	15 PLAINS	Smooth plains	TBD	TBD	TBD	TBD	TBD
	16 LIMB	Limb soan	TBD	TBD	TBD	TBD	TBD
	17 VALHAL	Valhalla multi-ring structure region	55	92	62	41	204
Clo	18 PALIMP	Valhalla palimpsest scan	0.34	14	19	57	408
	19 VRINGS	Valhalla ring transact	6	76	44	47	204
	20 CATENA	Crater chain in Valhalla	13	81	71	68	204
	21 LIMB	Limb scan	TBD	TBD	TBD	TBD	TBD
	22 EPLAINS	Smooth plains region	TBD	TBD	TBD	TBD	TBD
	23 GLOBAL	Global context map	100	87	94	62	204

FIG. 1

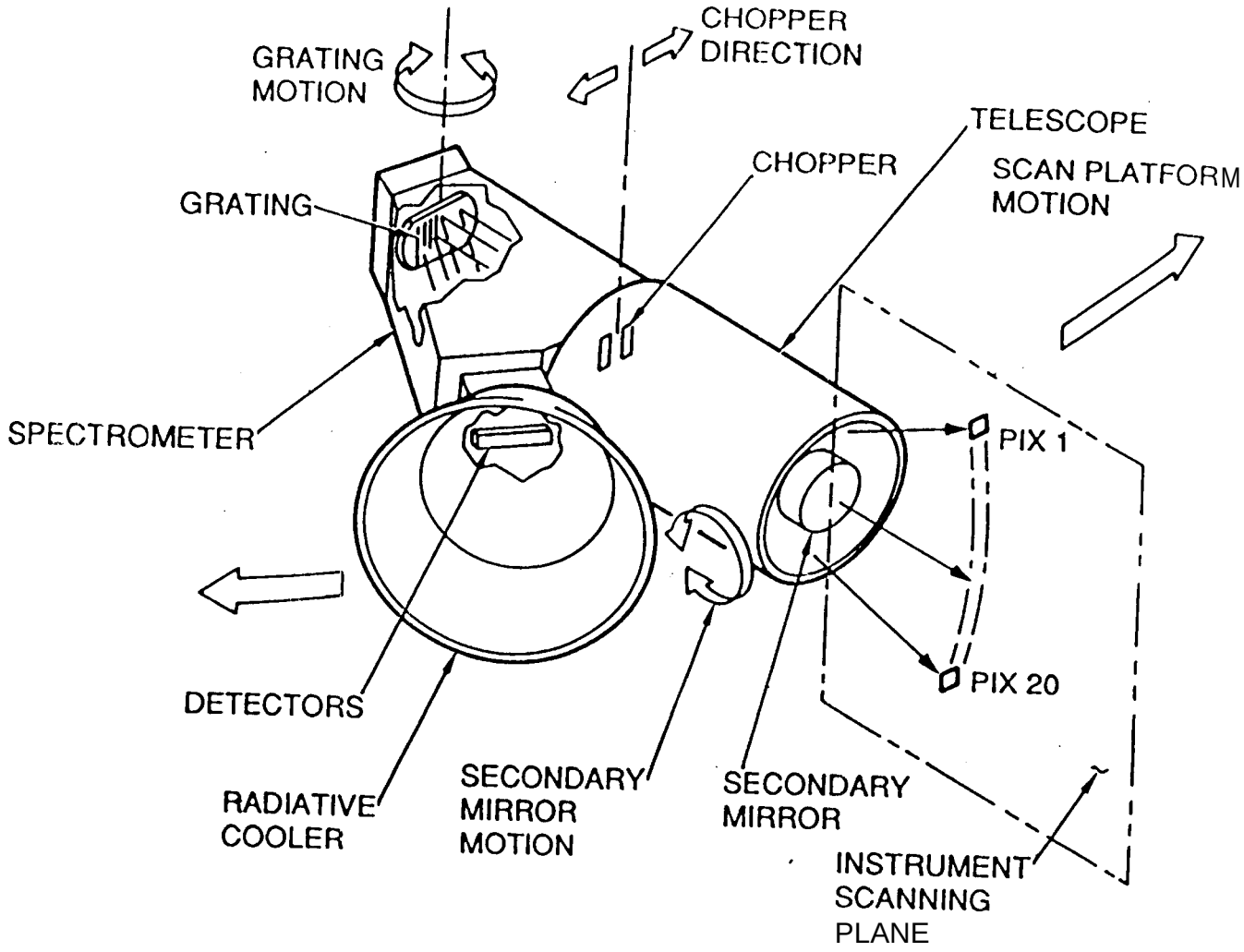
GRATING MOTION
CHOPPER DIRECTION
TELESCOPE
CHOPPER
SCAN PLATFORM MOTION
GRATING
SPECTROMETER
PIX 1
PIX 20
DETECTORS
RADIATIVE COOLER
SECONDARY MIRROR MOTION
SECONDARY MIRROR
INSTRUMENT SCANNING PLANE

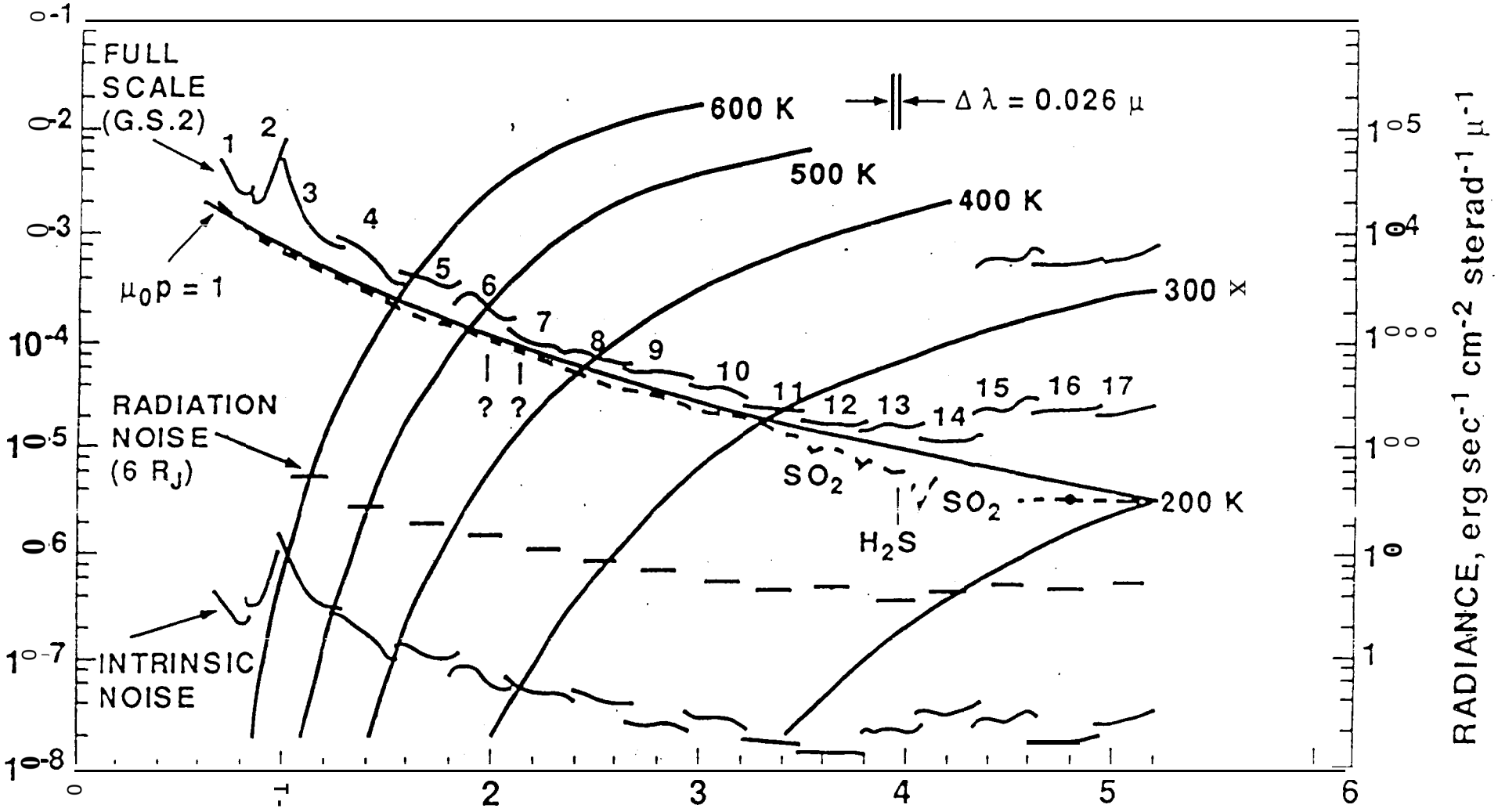
FULL SCALE (G.S.2)
600 K
500 K
400 K
300 K
200 K
Δ λ = 0.026 μ
μ0p = 1
RADIATION NOISE (6 RJ)
INTRINSIC NOISE
SO2
SO2
H2S
? ?
RADIANCE, erg sec-1 cm-2 sterad-1 μ-1

FIG 2

F G 3a

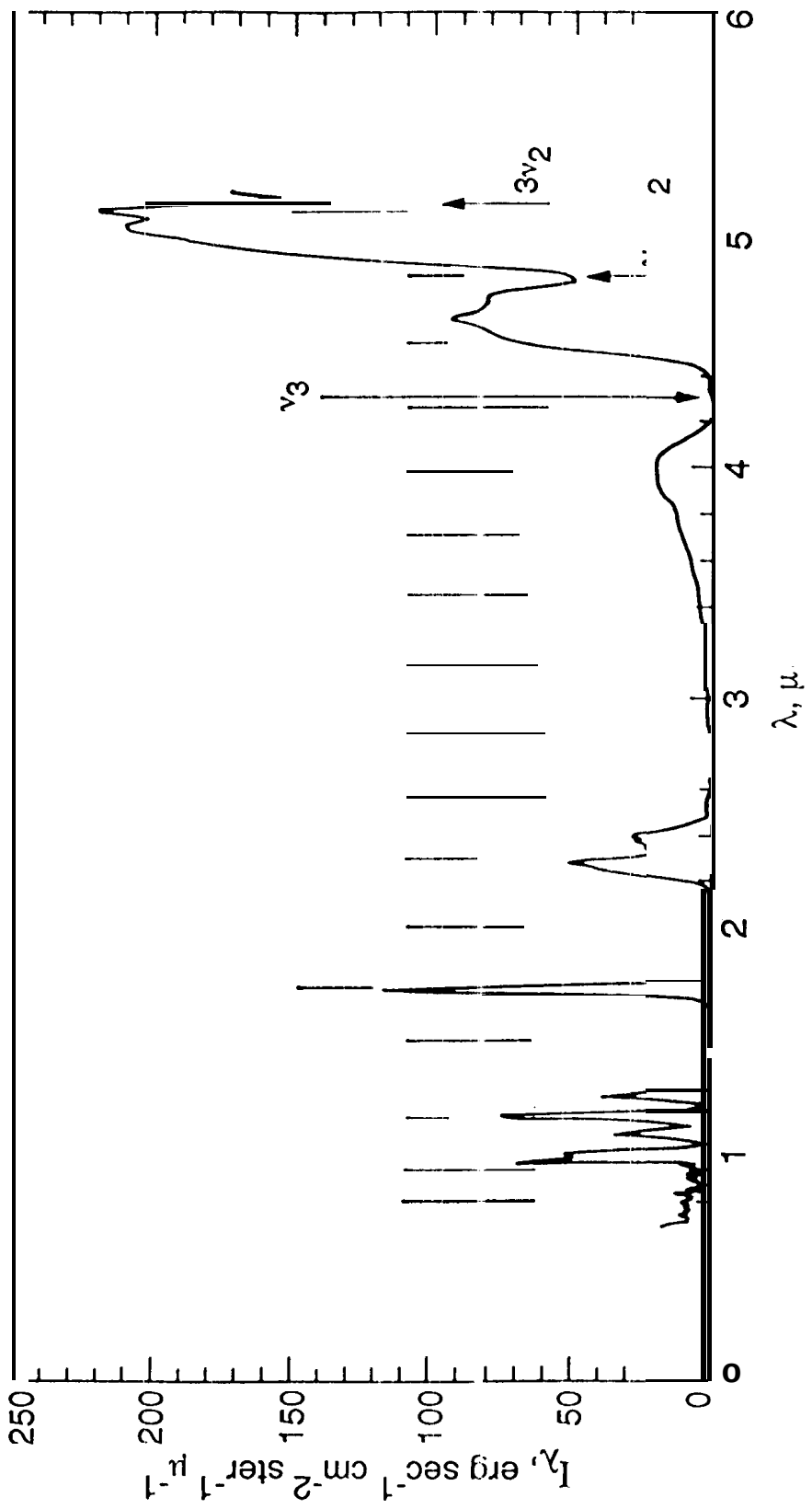
I_λ, erg sec^{-1} cm^{-2} ster^{-1} μ^{-1}
250
200
150
100
50
0
0
1
2
3
4
5
6
λ, μ
ν_3
$3\nu_2$
2

FIG 3b

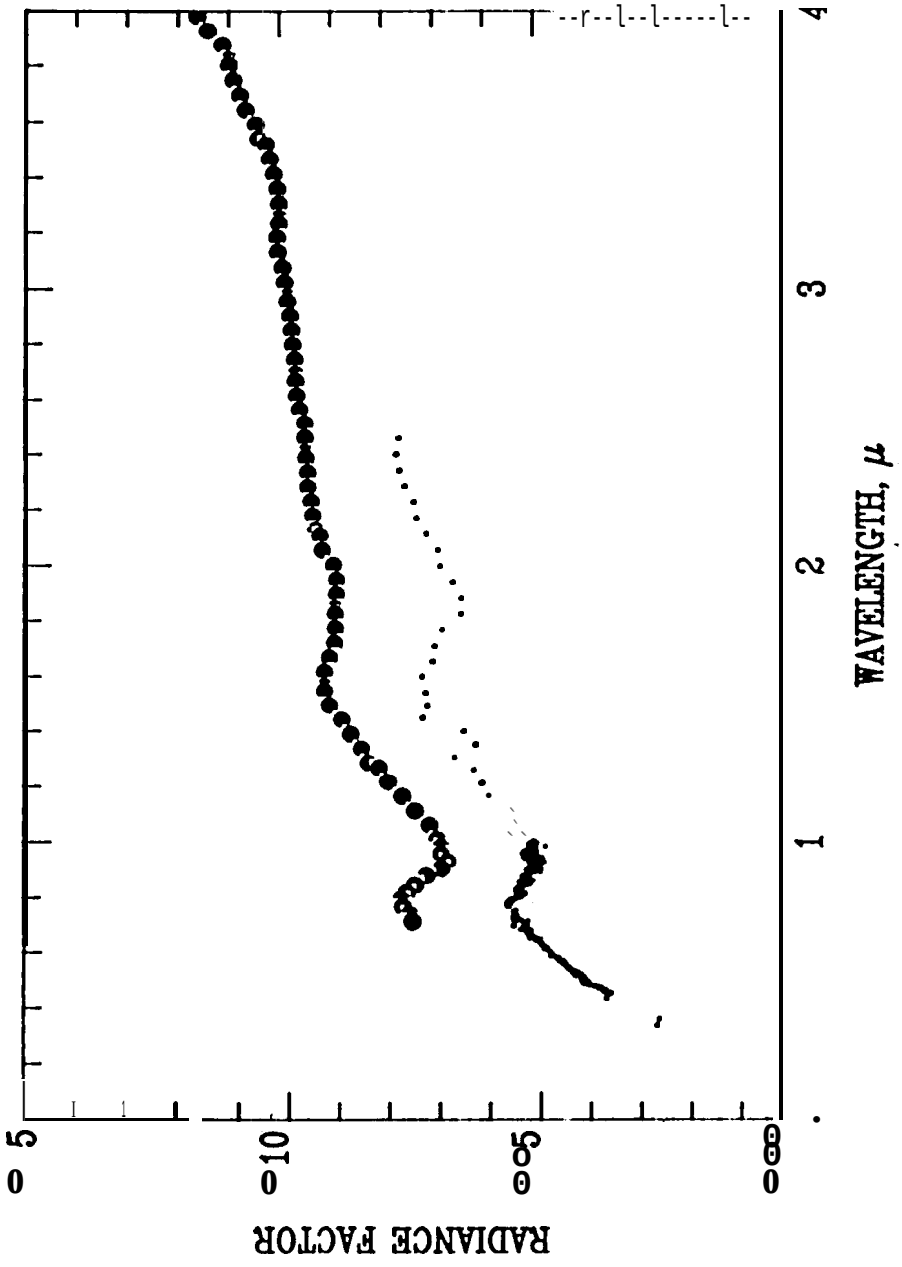

FIG 4

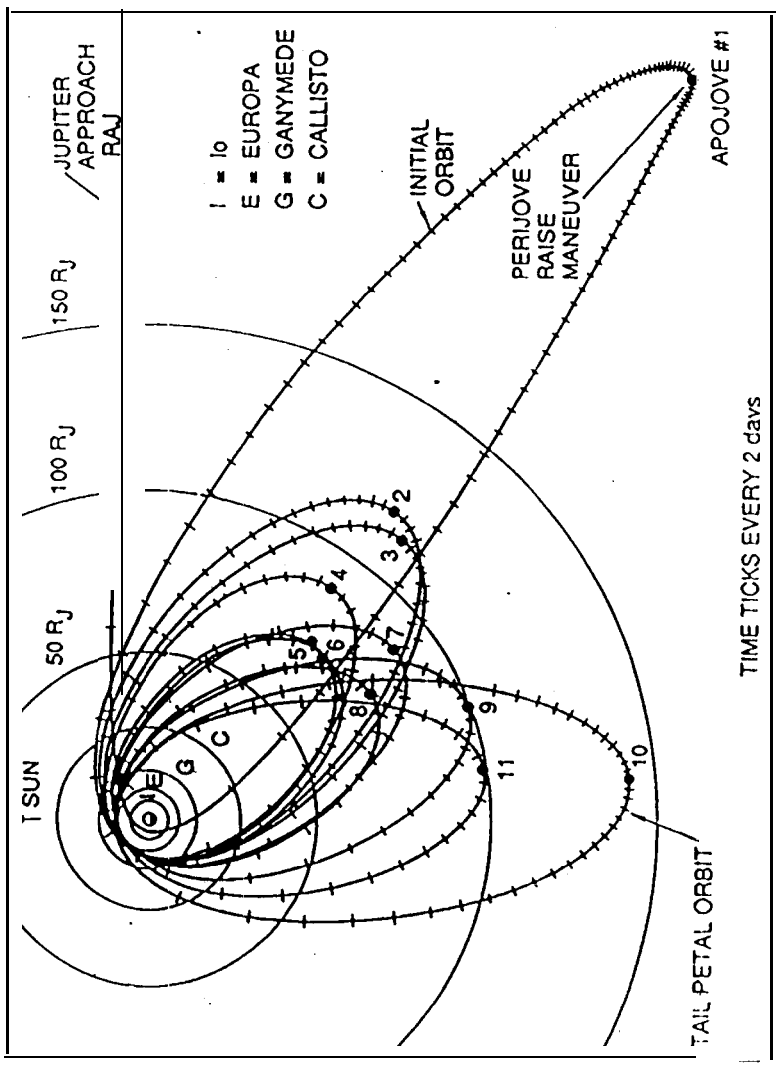
T SUN
50 R_J
100 R_J
150 R_J
JUPITER APPROACH RAJ
I = Io
E = EUROPA
G = GANYMEDE
C = CALLISTO
INITIAL ORBIT
PERIJOVE RAISE MANEUVER
APOJOVE #1
TIME TICKS EVERY 2 days
TAIL PETAL ORBIT
1
2
3
4
5
6
7
8
9
10
11

FIG 5

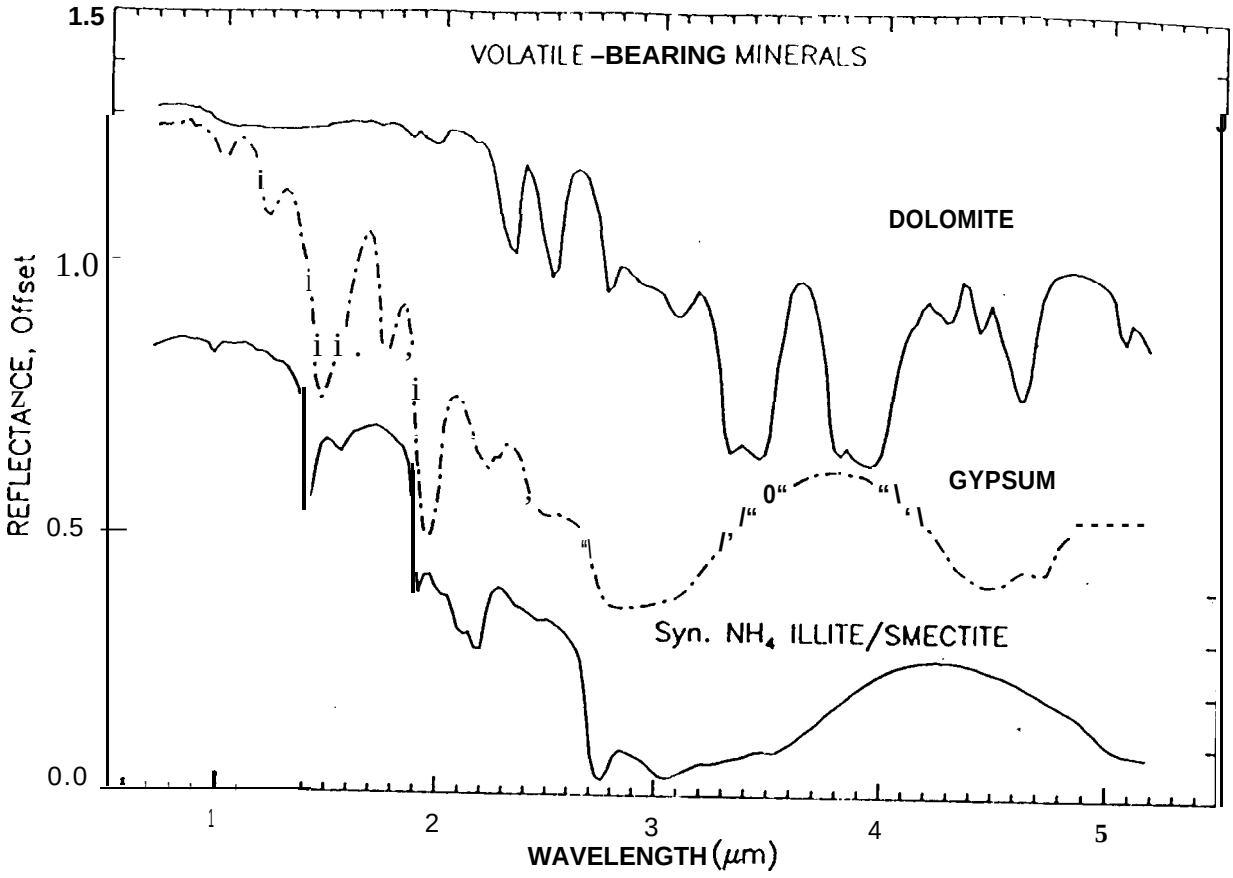
VOLATILE –BEARING MINERALS
DOLOMITE
GYPSUM
Syn. NH4 ILLITE/SMECTITE
REFLECTANCE, Offset
1.5
1.0
0.5
0.0
1
2
3
4
5
WAVELENGTH (μm)

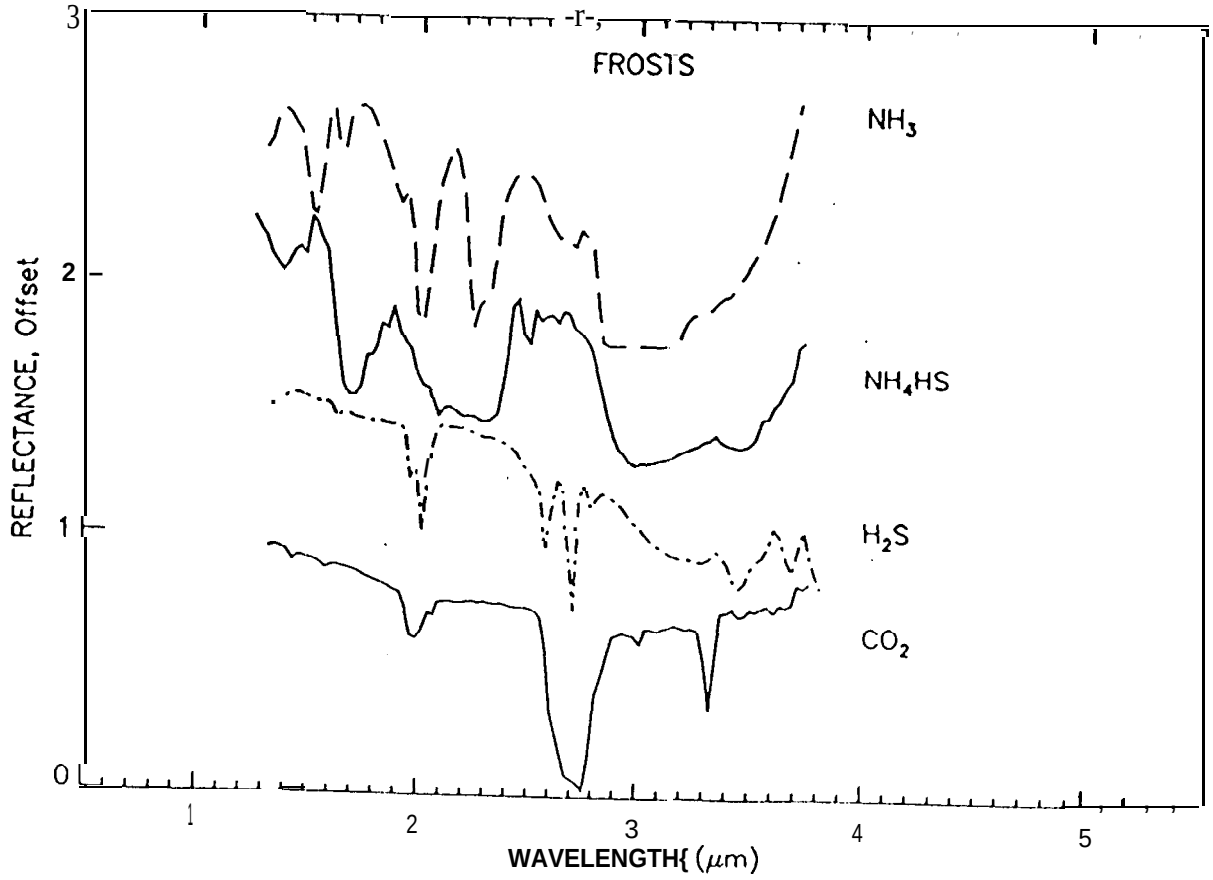
FROSTS
NH3
NH4HS
H2S
CO2
REFLECTANCE, Offset
3
2
1
0
1
2
3
4
5
WAVELENGTH (μm)

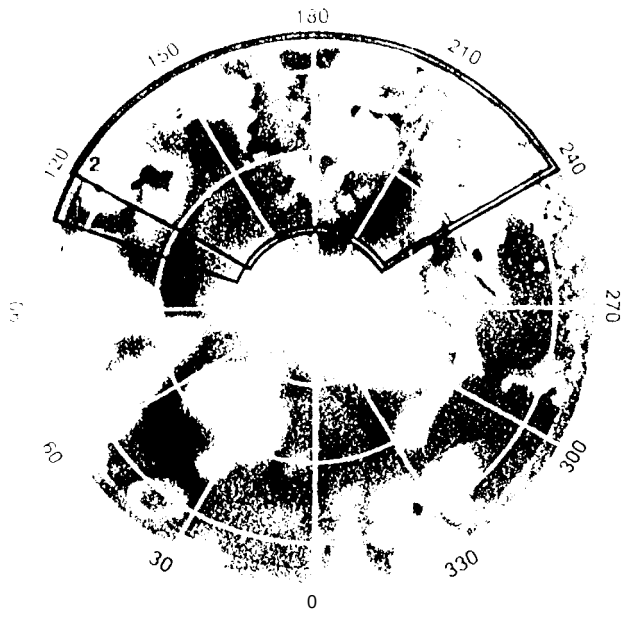

NORTH POLAR REGION

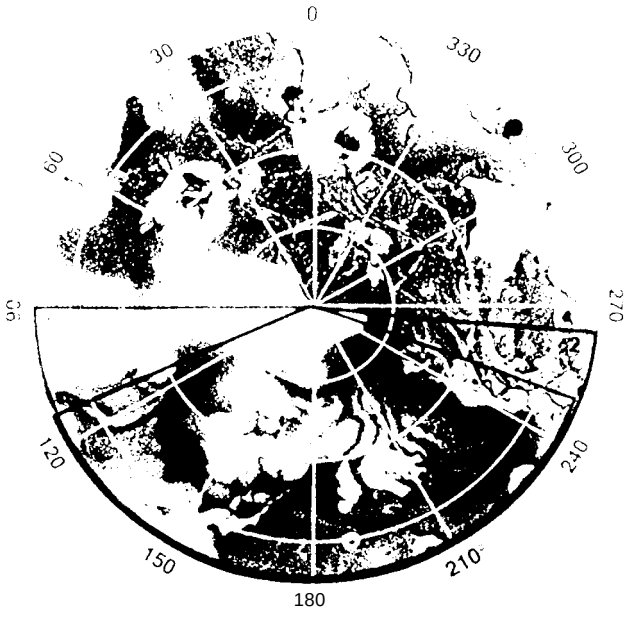

SOUTH POLAR REGION

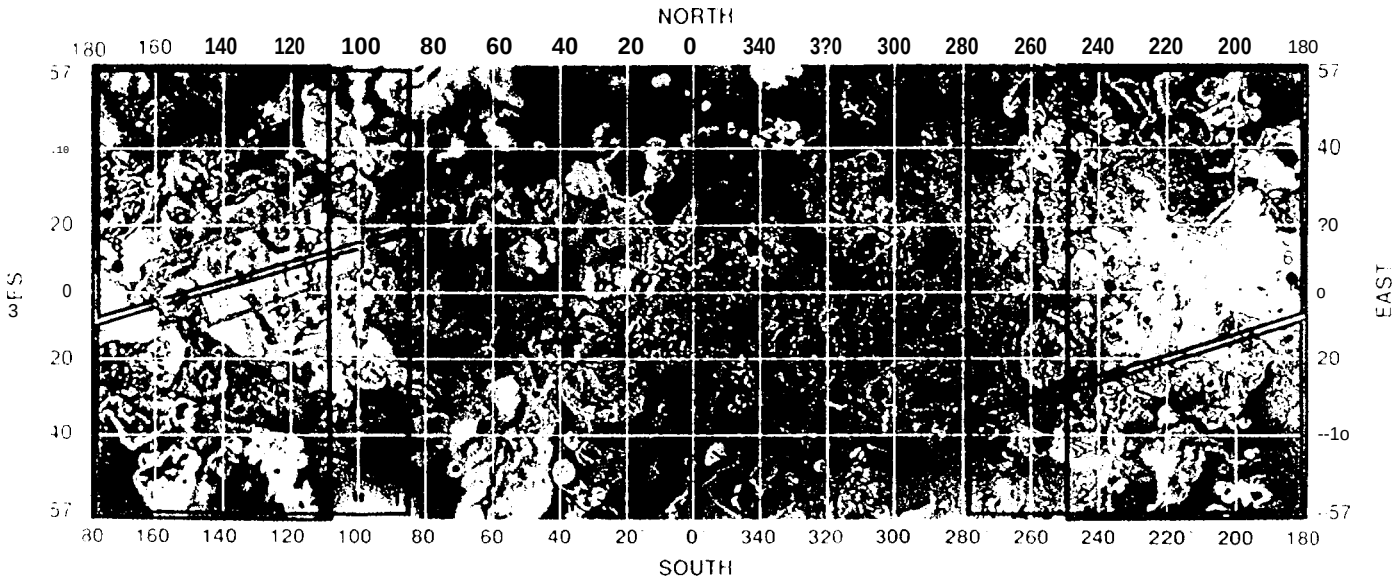

GLOBAL COVERAGE:

ORBIT (330) (370) (450) (730) (435) (340) (315)
(315) [330] (370) (455) (730) (435) (340)
220) (250) (330) (600) (430) (280) (240) (220)
(430)
(120) (140) (210) (440) (410) (200) (140) (120)
140) (120) (900) (900) (410) (200)
160) (180) (250) (510) (370) (210) (170) [160]
200 (830) (370)
408 (220) (300) 580) (350) (240) (210) (200)
(780) (345)
480) (510) (620) (930) (570) (500) (480)
(620) (930) (570) (540) (500) (480) (510) (620
600) (320) (350) (450) (715) 420) (330) (300)
330) 300 320 360) (715) (420)
150 (210) (370) (630) (510) (250) (180) (160)
160 150) (510)

EUROPA

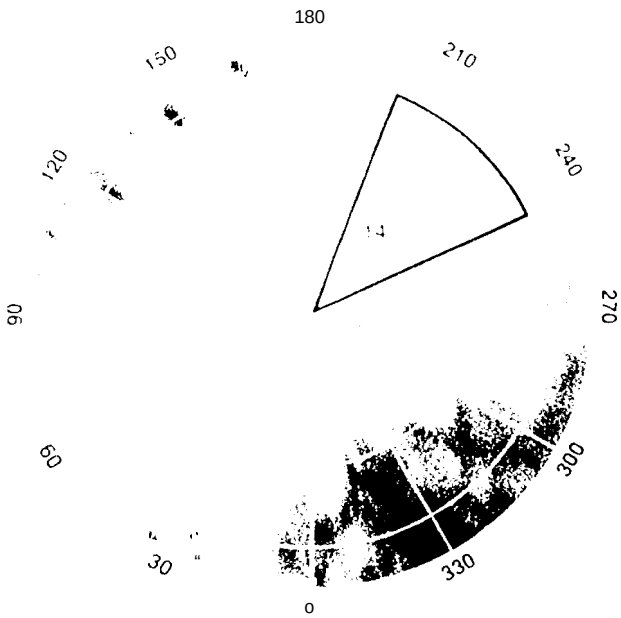

NORTH POLAR REG1ON

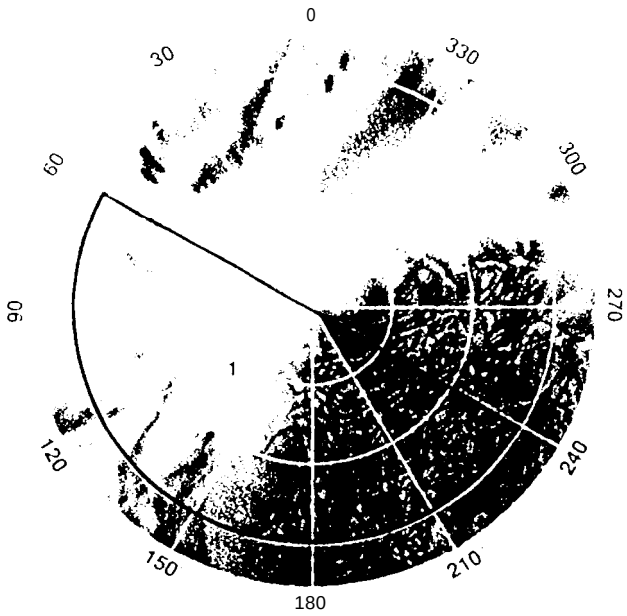

SOUTH POLAR REGION

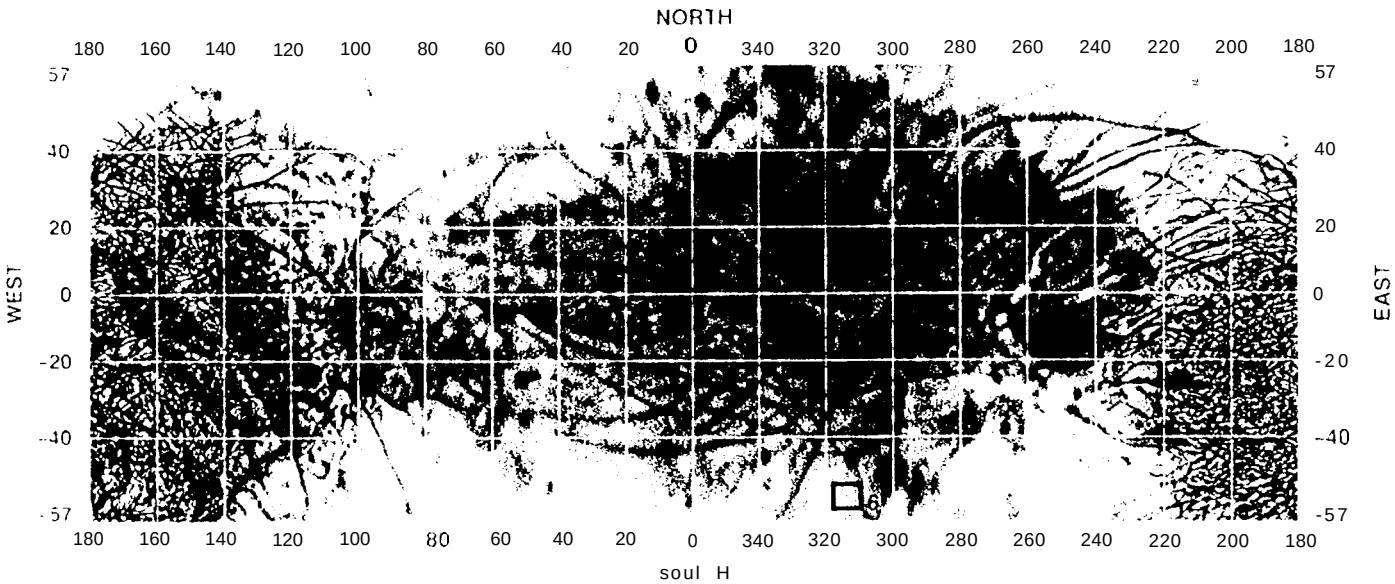

GLOBAL CO VERAGE:

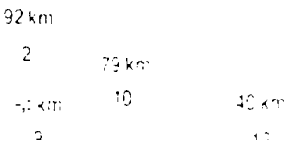

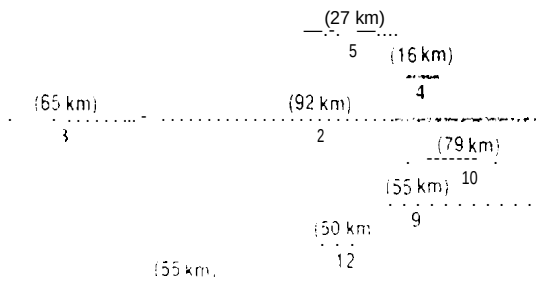

GANYMEDE

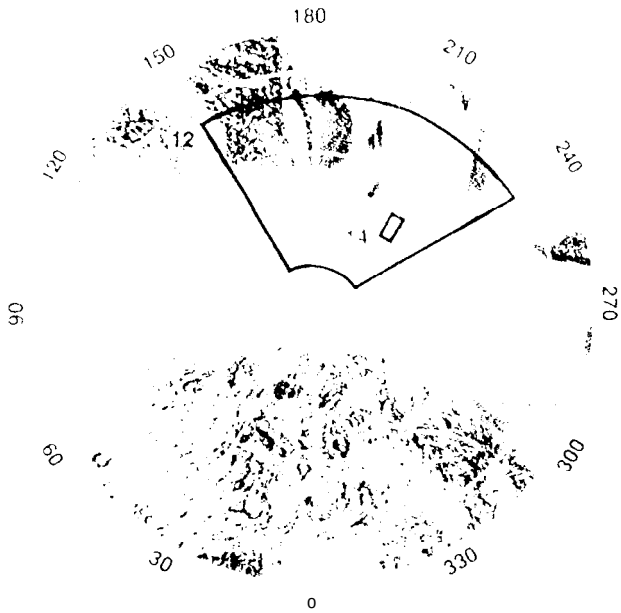

NORTHPOLARRE GION

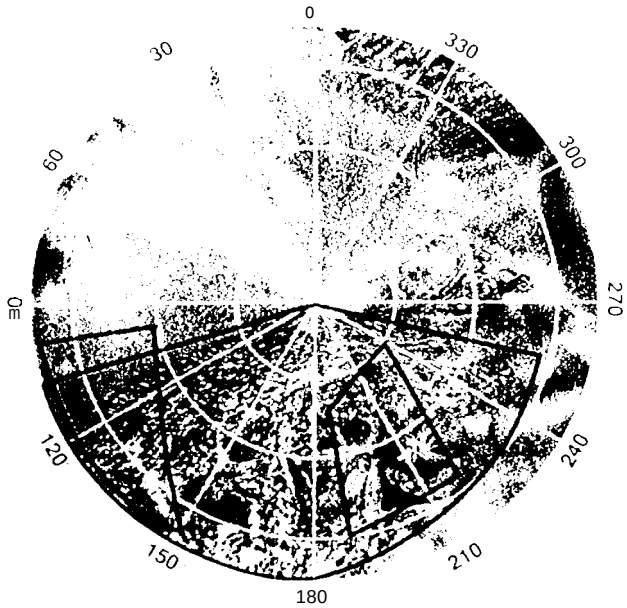

SOUTH POLARREGION

NOR1 t{

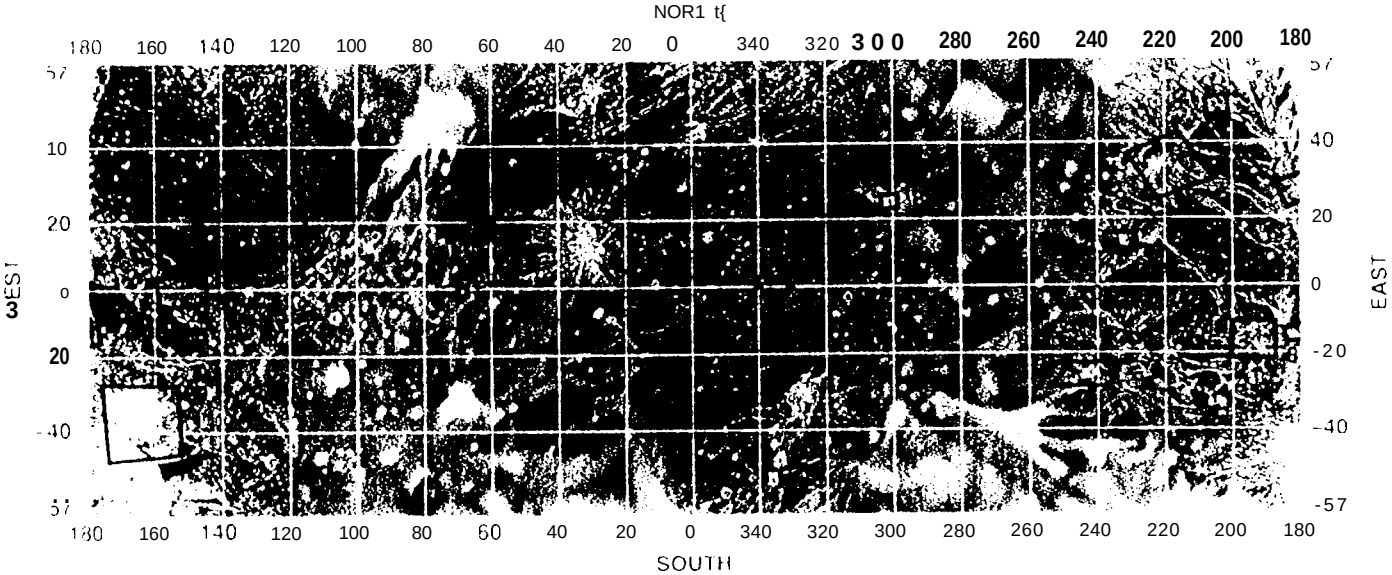

GLOBAL COVERAGE

(114 km)
1

(107 km)
15

(111 km)
18

28

(85 km)
28

(32 km)
30

CALLISTO

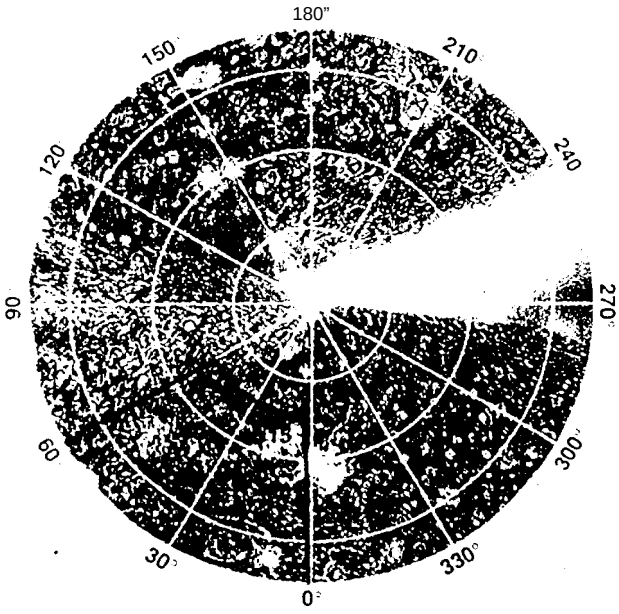

NORTH POLAR REGION

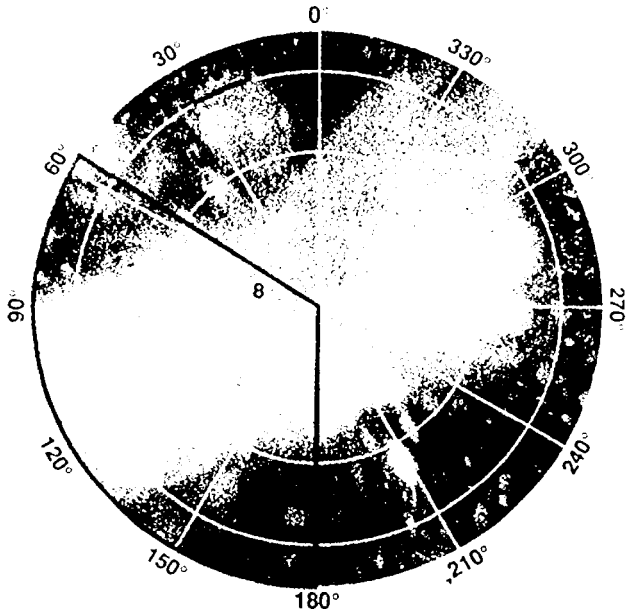

SOUTH POLAR REGION

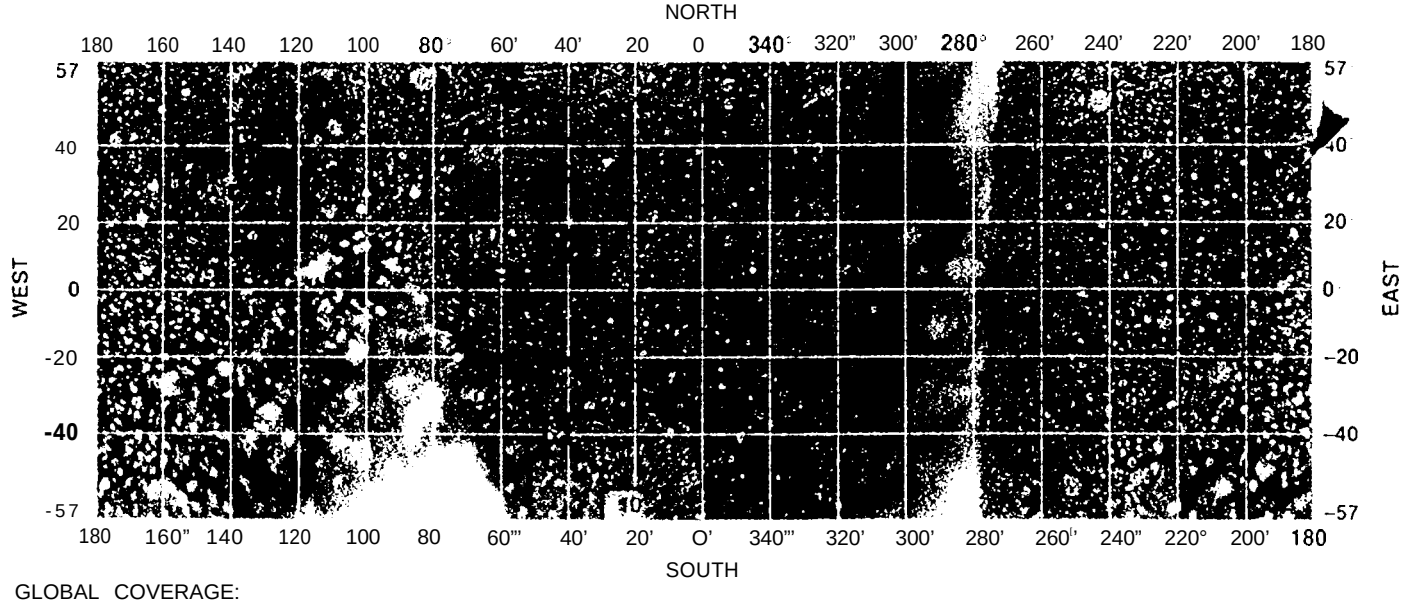

GLOBAL COVERAGE:

(955 km)
1
(211 km)
2
(-120 km)
3 (.100 km) (SOUTH POLE FLYBY)
11
(-100 km)
12
(110 km)
24